Review Article

Monitoring of the right ventricular responses to pressure overload: prognostic value and usefulness of echocardiography for clinical decision-making

Michael Dandel^

German Centre for Heart and Circulatory Research (DZHK), Partner Site Berlin, Berlin, Germany

Correspondence to: Michael Dandel, MD, PhD. Associated Professor of Medicine, German Centre for Heart and Circulatory Research (DZHK), Partner Site Berlin, Potsdamer Str. 58, 10785, Berlin, Germany. Email: mdandel@aol.com.

Abstract: Regardless of whether pulmonary hypertension (PH) results from increased pulmonary venous pressure in left-sided heart diseases or from vascular remodeling and/or obstructions in pre-capillary pulmonary vessels, overload-induced right ventricular (RV) dysfunction and its final transition into right-sided heart failure is a major cause of death in PH patients. Being particularly suited for non-invasive monitoring of the right-sided heart, echocardiography has become a useful tool for optimizing the therapeutic decision-making and evaluation of therapy results in PH. The review provides an updated overview on the pathophysiological insights of heart-lung interactions in PH of different etiology, as well as on the diagnostic and prognostic value of echocardiography for monitoring RV responses to pressure overload. The article focuses particularly on the usefulness of echocardiography for predicting life-threatening aggravation of RV dysfunction in transplant candidates with precapillary PH, as well as for preoperative prediction of post-operative RV failure in patients with primary end-stage left ventricular (LV) failure necessitating heart transplantation or a LV assist device implantation. In transplant candidates with refractory pulmonary arterial hypertension, a timely prediction of impending RV decompensation can contribute to reduce both the mortality risk on the transplant list and the early post-transplant complications caused by severe RV dysfunction, and also to avoid combined heart-lung transplantation. The review also focuses on the usefulness of echocardiography for monitoring the right-sided heart in patients with acute respiratory distress syndrome, particularly in those with refractory respiratory failure requiring extracorporeal membrane oxygenation support. Given the pathophysiologic particularity of severe acute respiratory syndrome coronavirus (SARS-CoV-2) infection to be associated with a high incidence of thrombotic microangiopathy-induced increase in the pulmonary resistance, echocardiography can improve the selection of temporary mechanical cardio-respiratory support strategies and can therefore contribute to the reduction of mortality rates. On the whole, the review aims to provide a theoretical and practical basis for those who are or intend in the future to be engaged in this highly demanding field.

Keywords: Echocardiography; right ventricle; right ventricle-pulmonary arterial uncoupling (RV-PA uncoupling); pulmonary hypertension (PH); right heart failure (RHF)

Submitted Sep 18, 2023. Accepted for publication Dec 10, 2023. Published online Feb 01, 2024.
doi: 10.21037/cdt-23-380
View this article at: https://dx.doi.org/10.21037/cdt-23-380

^ ORCID: 0000-0002-7131-9057.

Introduction

Regardless of whether pulmonary hypertension (PH) results from an increase in pulmonary venous pressure in left-sided heart diseases, or by pulmonary vascular remodeling and/or obstruction in the precapillary pulmonary vasculature, progression of overload-induced right ventricular (RV) dysfunction and its final transition into right-sided heart failure (HF) usually remains one of the main causes of mortality associated with PH (1-3). Both limited adaptation of RV function to increased afterload and the hardly predictable transition of adaptive responses into pathological maladaptive remodeling necessitate a close monitoring of the right-sided heart (2,3). Being particularly suited for close non-invasive monitoring of the right-sided heart, routine echocardiography becomes mandatory for the surveillance of patients with severe PH, and also highly beneficial in both the therapeutic decision-making and the evaluation of therapy results (4-8).

This article provides an overview on the current state of knowledge on the pathophysiological insights of heart-lung interactions with relevant impact on the clinical management of patients with PH of different etiology, as well as the diagnostic and prognostic value of echocardiography for monitoring the RV responses to pressure overload. Particular consideration is given to the usefulness and limitations of echocardiography for the prediction of life-threatening aggravation of RV dysfunction in transplant (Tx) candidates with precapillary PH, as well as the preoperative prediction of postoperative RV failure (RVF) in patients with primary end-stage left ventricle (LV) failure necessitating heart transplantation (HTx) or a LV mechanical support by an assist device (LVAD). In Tx candidates with severe refractory pulmonary arterial hypertension (PAH), a reliable prediction of impending RV decompensation can contribute to reduce both the mortality risk on the Tx list and the early post-Tx complications caused by severe RV dysfunction, and also to avoid the necessity of combined heart and lung Tx (8). In addition, the review will also focus on the clinical value of closely monitoring of the right-sided heart by echocardiography in patients with acute respiratory distress syndrome (ARDS), particularly in those with refractory respiratory failure requiring extracorporeal membrane oxygenation (ECMO) support. Given the pathophysiologic particularities of severe acute respiratory syndrome coronavirus (SARS-CoV-2) pulmonary infection, characterized by a high prevalence of a widespread thrombotic microangiopathy associated with increasing flow resistance in the pulmonary circulation and afterload-induced RV dysfunction, it is not surprising that in coronavirus disease (COVID-19) related ARDS, RV dilation and dysfunction were found independently associated with a significant increase in mortality risk (9-12). In patients with refractory COVID-19-related ARDS, echocardiography can improve the selection of temporary mechanical support strategies (e.g., veno-venous ECMO, veno-arterial ECMO or even veno-arterial ECMO plus temporary mechanical RV support) (10,13).

Ventricular myocardial pump function

Right versus left ventricle: common features and particularities

Optimal heart function depends mainly on cardiac myocyte contractile abilities and the hemodynamic load that needs to be overcome (i.e., preload and afterload), but is also affected by valvular function, ventricular interdependence, synchrony of myocardial contraction, cardiac rhythm, and pericardial restriction (2,3,13).

Providing sufficient cardiac output (CO) to maintain an optimal blood flow to all organ systems is the primary function of the LV, whereas the primary of role RV function is to sustain an effective CO by minimizing the impedance to systemic venous return to the heart while also not limiting LV filling (14).

Systolic ventricular failure can be induced by both cardiac diseases and overload. Initially, the increasing stretching of myocardial fibers induced by the rising intraventricular end-diastolic pressure (EDP) as a consequence of stroke volume (SV) reduction, initiates important compensatory responses like increase in myocardial contraction force (Frank-Starling Law) and cardio-myocyte hypertrophy (3,15,16). Additionally, neurohormonal responses to the reduced CO aiming at maintaining the perfusion of vital organs (especially sympathetic activation and renin-angiotensin-aldosterone system activation associated with an increase of the systemic vascular resistance and the renal salt and water retention, respectively), act initially also as compensatory measures (16,17). However, continuous ventricular overloading will ultimately trigger the development of a pathologic (maladaptive) remodeling with ongoing deterioration of systolic function accompanied by ventricular geometry alterations, as well as by a rise in ventricular wall stiffness (16-18). With the advancement of geometry alterations, the

ventricle must generate correspondingly higher wall tension to preserve the systolic pressure in order to prevent further reduction of the CO. However, the higher wall tension reduces the coronary blood flow and increases at the same time the energy expenditure of the overloaded ventricle (17,18). Ventricular size and geometry changes also cause atrioventricular valve ring changes with subsequent secondary regurgitation associated with aggravation of ventricular volume overloading and further reduction of the forward stroke volume (SV_f) (18). Ventricular overstretching also overrides the Frank-Starling adaptive response and triggers a continuous reduction of ventricular compliance, thus generating also a progressive diastolic malfunction accompanied by substantial aggravation of both the clinical phenotype and the severity of ventricular dysfunction (17,18). Therefore, with disease progression, both systolic and diastolic dysfunction, contribute in an interconnected manner to the severity and the progression and of ventricular failure.

When assessing the RV, certain anatomical and functional particularities, especially its irregular shape and inhomogeneous contraction should be considered, because the RV is anatomically and functionally quite different from the LV (19). Thus, the three anatomical RV components (i.e., inlet, outlet and apex) contribute differently to the ejection. In addition, the heterogeneity regarding the ventricular mechanics (including its timing), even in healthy persons, complicates the RV investigations (16). Given the existence of a relevant ventricular interdependence, the RV pump function is also related to the LV function. Thus, via the crista supraventricularis which enables the transmission of the ventricular septum contraction to the RV free wall (RVFW) with simultaneous narrowing of the tricuspid valve (TV) ring, the LV contraction promotes both the RV pump function and the TV competence (19,20). Thanks to this interdependence, the LV can contribute for about 30% of systolic pressure generation in the RV, and LV contraction can generate up to 40% of both RV-SV and pulmonary flow (19,20). Being mainly a "volume pump", the compliant RV with his particularly thin walls tolerates better volume overload than pressure load and is therefore, compared to the LV, much more sensitive to high afterload (16,19). Because of the particularly high load dependency of RV pump function, the pressure overloading-induced spherical dilation associated with high wall tension induced reduction of coronary blood flow with consequent systolic dysfunction arise much earlier in the RV than in the LV (8,19). The fact that differently from the LV the RV coronary blood flow occurs during the systole and not during the diastole also contributes to the much less adaptability of the RV to increased afterload (14).

Because of the different orientation of myocardial fibers in the RV inflow and outflow region, these two regions contract perpendicularly to each other (i.e., longitudinally at the inflow part and circumferentially at the outflow part) (3,16). Because, overall, the RV myocytes are predominantly oriented longitudinally, the RV contraction pattern is normally characterized by a mainly longitudinal shortening (14,16,20). Thus, the longitudinal shortening of the subendocardial myocytes accounts for about 75% of normal RV contraction (21). Whereas early RV-pulmonary arterial (RV-PA) uncoupling is associated with reduced longitudinal function, advanced RV-PA uncoupling appeared associated with a risk-related reduced anteroposterior RV wall movement due to the higher contribution of the circumferentially orientated myocardial fibers in the outflow part (22). All this explains the reduced adaptive capacity to increased afterload of the RV in comparison to the LV. From a physiological point of view, this more reduced adaptability is essential for ensuring the appropriate „matching" of RV and LV outputs because any discrepancy, no matter how small, cannot be sustained. Even a short-term higher RV output, meaning that more blood will be introduced into the pulmonary vasculature than it will be removed can have immediate life-threatening consequences, depending on the extent of the mismatch.

Diastolic function also differs between the ventricles. In comparison to the LV, the thinner RV walls are more distensible and their higher compliance allows relatively large changes in the RV volume without functionally relevant changes in the filling pressure (19,20).

Right ventricle responses to pressure overload

Under normal conditions, the RV coupling with the pulmonary circulation, which is necessary for maintaining a continuous adequate blood flow in the pulmonary arteries, occurs in an energy efficient manner due to the low resistance to blood flow in the highly compliant low pressure pulmonary circulation (19).

RV adaptation to pressure overload depends on the intrinsic RV myocardial contractility, the adaptability of the myocardium to sustained abnormally high wall stress, as well as the progression rate (e.g., chronic steadily increase or acutely occurring massive increase in the resistance against blood flow in the lung vessels), duration and severity of the

pressure overloading (5,19). The early adaptation response to ongoing pressure overload is mainly realized by an increase in myocardial mass and contractility (i.e., adaptive hypertrophy) enabled by an upregulation of subcellular organelles (e.g., sarcolemma, sarcoplasmic reticulum, myofibrils, and mitochondria), which aimed to minimize the wall stress for the RV undergoing an abnormally high workload (homeometric adaptation) (3,23). In this adaptive state, RV-PA coupling, CO, ejection fraction (EF), and exercise capacity are maintained (3). However, myocyte hypertrophy leads to increased RV diastolic pressure, which indicates that increased RV contractile function occurs at the cost of an alteration of its diastolic function (3). The progression of pressure overloading eventually exhausts the homeometric adaptation and induces a transition of the RV to a heterometric "adaptation" where the RV dilates and uncoupling occurs because its contractility fails to match the afterload (3).

In the course of time, there were identified various stages of adaptive and maladaptive RV remodeling. The maladaptive RV remodeling passes through further stages of reversible and irreversible RVF. The adaptive and maladaptive myocardial changes are not completely different reactions to overloading. There seems to be a succession of different phases during the course of RV adaptation before its adaptability becomes exhausted (24). However, the basic pathophysiological processes involved in the transition toward RVF are not fully clarified.

Several processes have been associated with either adaptive or maladaptive RV phenotypes (e.g., capillary rarefaction, metabolic shift from oxidative metabolism toward glycolysis and sympathetic hyperactivity, and fibrosis). In end-stage RVF, experimental data suggest a larger contribution of interstitial fibrosis to total stiffness, whereas cardiomyocyte stiffening may play a larger role in earlier stages (25). Prolonged activation of adaptive mechanisms, particularly in association with a progressive increase of hemodynamic overloading, eventually leads to RV diastolic stiffness, mitochondrial dysfunction, and ischemia, followed by irreversible RVF. Given that the adaptability of the right ventricle to high afterload varies greatly among different patients, the transition to right-sided HF remains difficult to predict (24).

After full exhaustion of its adaptive abilities to overcome the persistently high resistance in the pulmonary circulation, the RV responses to high afterload exhibit more often a transition to pathological myocardial hypertrophy associated with a decrease in myocardial blood supply due to the reduced capillary density, plus downregulation of the above mentioned subcellular activities. Ca^{2+}-handling abnormalities, oxidative stress, inflammation, and cardiomyocyte apoptosis appeared critically involved in the depression of contractile function in patients with pathological hypertrophy (23,26).

The adaptability of a pressure overloaded RV is mainly reflected by its ability to develop high systolic pressures without relevant alterations in its cavity size and geometry (8,27). As long as a pressure overloaded RV with reduced output remains able to increase significantly its systolic pressure in response to increased afterload, without relevant geometry alterations and/or aggravation of a preexisting tricuspid regurgitation (TR) grade ≤2, its adaptability to afterload increase is preserved, and the reduction of its afterload can normalize the output (5,27). Thus, even in the presence of severe secondary RVF, patients with end-stage refractory LV failure who necessitate a LVAD support usually do not need a long-term biventricular VAD (BiVAD) support before the adaptability of the RV to high afterload becomes irreversibly impaired by ongoing maladaptive structural and functional alterations (27-29). *Figure 1* shows the major pathophysiologic steps during the development of non-reversible secondary RVF in patients with advanced LV failure.

PH may be initially postcapillary (i.e., resulting from left-sided heart diseases-induced increase in pulmonary venous pressure), or precapillary (caused by continuous vasoconstriction and vascular remodeling in the distal pulmonary arterial tree) leading to increase in the pulmonary vascular resistance (PVR) (30). PH related to left HF [World Health Organization (WHO) group 2 PH] which is by far the most frequent form of PH worldwide (representing over 50% of all cases of PH) is the most common cause of secondary RVF (1,31,32). Starting as an isolated postcapillary PH, with aggravation of the left-sided HF and subsequent development of a reactive increase in the precapillary PVR, as soon as the latter becomes out of proportion to the increase in the pulmonary venous pressure, the PH will eventually turn into a combined precapillary and postcapillary PH associated with life-threatening biventricular HF (33). Among the precapillary PH types, the prognostically most relevant subtypes are the chronic thromboembolic PH and the PH caused by pulmonary artery obstructions (WHO group 4), the PH caused by lung diseases and hypoxemia (WHO group 3), and the less common but clinically highly important PAH subtypes belonging to the WHO group 1 (33). As shown

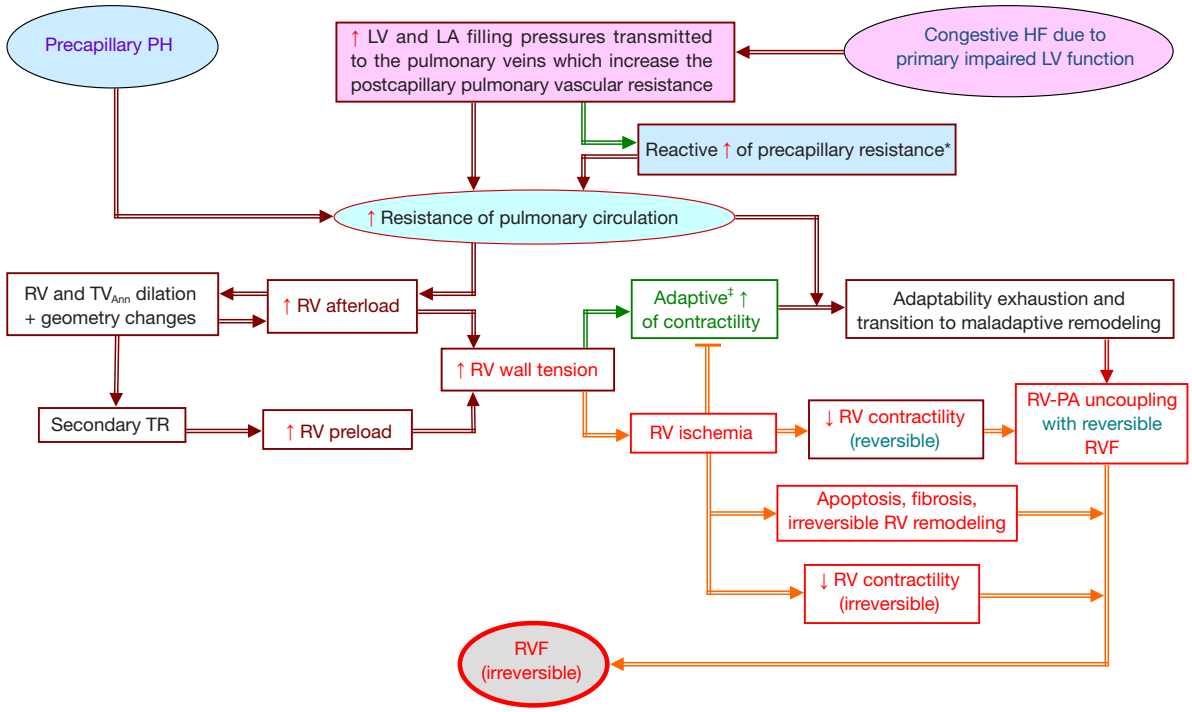

Figure 1 Major pathophysiological mechanisms involved in the development of high afterload-induced right ventricular failure. The arrows inside the boxes indicate increase (↑) or decrease (↓). Green lettering and green arrows in and outside the box indicate favorable (adaptive) responses. Blue-green lettering in the boxes indicates reversibility of alterations. *, initially a protective mechanism against pulmonary edema. ‡, Frank-Starling mechanism and adaptive myocardial hypertrophy. PH, pulmonary hypertension; LV, left ventricle; LA, left atrium; HF, heart failure; RV, right ventricle; TV_{Ann}, tricuspid valve annulus; TR, tricuspid regurgitation; RVF, RV failure.

in *Figure 2*, the pathophysiological mechanisms involved in the development of high afterload-induced RVF are similar, irrespective of the causes or the mechanisms that have contributed to the rise of the resistance to the blood flow in the pulmonary circulation. When assessing the RV overload in PH of different etiologies it is useful to consider in addition to the PVR also the contribution of other mechanical mechanisms involved in the RV pressure overloading like the dynamic opposition of the pulmonary circulation due to pulsatile blood pressure/flow (34). Experimental studies on the effect of PA collagen content on pulsatile RV afterload and on RV hypertrophy in early hypoxic PH revealed a significant correlation between pulse pressure and RV hypertrophy (34). In prevalent PAH patients, the severity of proximal PA remodeling is related to the risk stratification and associated with PA compliance and RV-PA coupling impairment beyond the indirect effect of the mean PA pressure (35).

In contrast to the above mentioned types of PH, where a not previously damaged RV can improve its pump function within certain limits allowing different degrees of adaptation to unphysiologically high afterload, in a relatively high proportion of patients with refractory COVID-19-related ARDS associated with an acute RV pressure overloading inducing widespread thrombotic microangiopathy, the RV becomes unable to provide a vitally necessary transpulmonary blood flow (10,36,37). This explains the high incidence of RV dilatation (up to 70%) in hospitalized patients, the high prevalence (up to 50%) of RV-PA uncoupling in patients necessitating intensive care, and the very high mortality rates (i.e., 54–85%) in patients with COVID-19-related ARDS (36,38-40).

Evaluation of the right ventricle by echocardiography

Since RV function was identified as an important prognostic predictor in congestive HF and PH of various etiologies

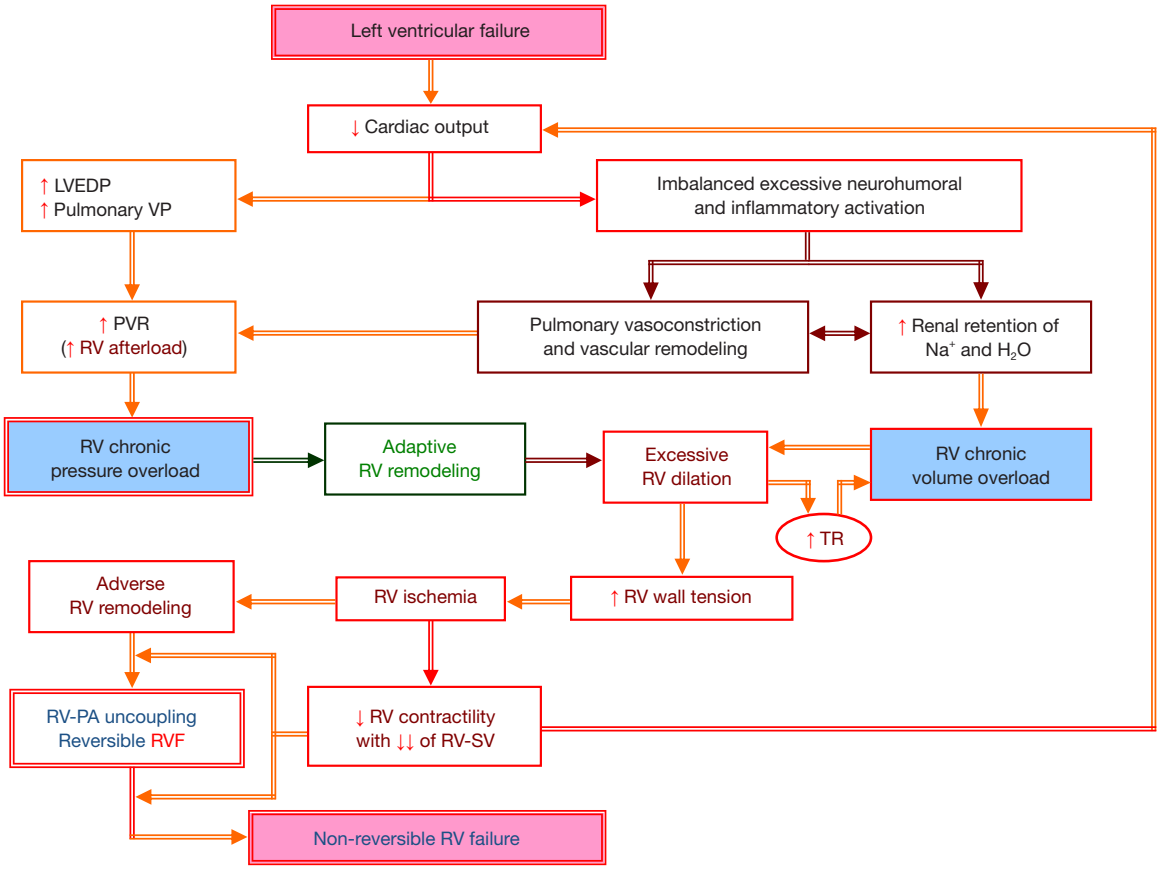

Figure 2 Key pathophysiologic steps in the development of non-reversible secondary right ventricular failure in patients with advanced left ventricular failure. The arrows inside the boxes indicate increase (↑) or decrease (↓). LVEDP, left ventricular end-diastolic pressure; VP, venous pressure; PVR, pulmonary vascular resistance; RV, right ventricle; TR, tricuspid regurgitation; PA, pulmonary artery; RVF, RV failure; SV, stroke volume.

and, in particular, since durable mechanical assistance of the LV has been more frequently used as a vital therapy for end-stage HF, comprehensive evaluation of the right-sided heart has gained a growing importance. At the present time echocardiography is one of the major tools for the assessment of the right-sided heart. It should be considered, however, that RV morphological and functional alterations cannot be evaluated simply by extrapolating the expertise obtained from the more intensive echocardiographic assessment of the LV, because of specific challenges and limits related to the RV assessment by this important non-invasive technique. Due to the complex 3-dimensional RV shape and the limited imaging window, the poor definition of its endocardial surface, the differing complexity of the contraction-relaxation mechanism among the main RV anatomical components the influence of LV size, geometry and function on RV anatomy and pump function, plus the characteristically high sensitivity of the RV its loading conditions, accurate interpretations of echocardiographic findings remained quite challenging. *Table 1* gives an overview of the normal values for the major echocardiographic parameters used for evaluations of right atrial (RA) and RV geometry, size and function (41-45).

Assessment of RV size and geometry

Due to its anatomical particularities and because its dilation can take place both globally and regionally, the assessment of the RV by transthoracic echocardiography (TTE) necessitates in addition to the standard views also the use of certain specific short and long axis views.

The apical 4-chamber view is essential for RV size

Table 1 Normal values of the major echocardiographic parameters used for the evaluation of right atrial and right ventricular size, geometry and function (41-45)

Echocardiographic parameters	Normal values	
	Men	Women
RV base/BSA (mm/m^2 BSA)	19.2±3.1	18.9±2.5
RV mid/BSA (mm/m^2 BSA)	16.1±3.2	15.2±2.7
RV length/BSA (mm/m^2 BSA)	39.0±4.8	40.6±5.0
RVOT prox. PLAX (mm)	33±5	31±4
RVOT prox. SAX (mm)	32±4	31±4
RVAdi (cm^2/m^2 BSA)	10.7±2.3	9.2±2.6
RVAsi (cm^2/m^2 BSA)	6.1±1.3	5.1±0.09
3D EDV (mL/m^2 BSA)	61.3±12.3	54.0±10.4
3D ESV (mL/m^2 BSA)	26.0±6.2	22.5±4.9
RV FAC (%)	43.0±4.0	44.3±4.0
	41.4±7.7	44.0±6.8
3D EF (%)	57.5±4.1	58.4±4.3
TAPSE (mm)	23.7± 4.1	22.5±4.3
	26±4	26±4
RVS' (cm/s)	14.7±2.6	13.6±2.3
2D-RVFWLS (%)	–26.7±5.2	–27.5±5.5
	–26.9 (–28.0 to –25.9)	
2D-RVGLS (%)	–21.7±3.4	–22.3±3.5
	–23.4 (–24.2 to –22.6)	
2D-RVFWLSR (s^{-1})	–1.58 (–1.88 to –1.29	
2D-RVGLSR (s^{-1})	–1.45 (–1.59 to –1.31)	
3D-RVFWLS (%)	–25.5 (–28.6 to –22.3)	
3D-RVGLS (%)	–21.3 (–24.6 to –17.9)	
RA area (cm²/m^2 BSA)	8.9±1.6	8.8±1.3
RA length (cm/m^2 BSA)	2.5±0.3	2.7±0.3
2D-RA strain (%)		
Reservoir phase	42.7 (39.4 to 45.9)	
Conduit phase	23.6 (20.7 to 26.6)	
Contraction phase	16.1 (13.6 to 18.6)	
2D-RA strain rate (s^{-1})		
Reservoir phase	2.1 (2.0 to 2.1)	
Conduit phase	–1.9 (–2.2 to –1.7)	
Contraction phase	–1.8 (–2.0 to –1.5)	
SPAP (mmHg)	23.2±4.4	

Data are presented as mean ± standard deviation or median (interquartile range). RV, right ventricle; BSA, body surface area; RVOT, RV outflow tract; PLAX, parasternal long axis; SAX, short axis; RVAdi, RV diastolic area index; RVAsi, RV systolic area index; EDV, end-diastolic volume; ESV, end-systolic volume; FAC, fractional area change; EF, ejection fraction; TAPSE, lateral tricuspid annulus peak systolic excursion; RVFWLS, RV free wall longitudinal strain; RVGLS, RV global longitudinal strain; RVFWLSR, RV global longitudinal strain rate; RVGLSR, RV global longitudinal strain rate; RA, right atrium; SPAP, systolic pulmonary arterial pressure.

measurements. However, these measurements necessitate an optimal visualization of the RVFW and the lateral TV ring. Therefore, dedicated RV-focused apical 4-chamber views become frequently indispensable, but it is necessary to maintain a true 4-chamber view in order to obviate the risk of measurements errors. In patients with normal LV size, the RV size can be roughly evaluated by the RV to LV area ratio (normal value: <0.66) (20). Subcostal views can be helpful in patients with inadequate apical images of the RV. However, the challenges in defining the RV antero-posterior plane from these views can generate incorrect measurements of RV size (20).

Parasternal views enable the measurements of the RV outflow tract (RVOT) but, in long-axis views, the measurements can vary up to 40%, depending on the patient position during the obtainment of the RVOT images (20). LV dilation can induce misguiding reductions in the visible RVOT size in the parasternal long-axis view by modifying its spatial position (rotation out of the section plane) (46). The RVOT measurements should therefore be performed in both parasternal views (i.e., long-axis and short-axis view). For RV dimensions and RV area measurements acquired in the apical 4-chamber view, as well as for the RVOT dimensions acquired in parasternal views, the recommended reference values for 2D-TTE-derived RV size measurements in adults reveal large differences between the lower and upper values (20,47). Measurements of RV size can also vary with slight rotation or tilting the transducer and should be therefore carried out only in the recommended standard views (46). However, the lack of accurate anatomic landmarks to define the RV standard views can induce both under- and overestimation of the actual RV size (46,47).

The lack of relevant options for reliable measurements of the RV end-systolic and end-diastolic volume (ESV and EDV, respectively) is a major limitation of 2D-echocardiography (46,47).

Because of their low reproducibility and poor reliability, RV volume estimations by 2D-echocardiography are not anymore recommended for practical utilization (20,47). Because 3D-echocardiography obviates geometric assumptions, 3D-TTE is more reliable for RV volume measurements. 3D-TTE-derived RV volume measurements showed good correlations with cardiac magnetic resonance imaging (MRI) derived RV volume calculations (20,48). Nevertheless, the 3D-TTE-derived reference values for RV normal EDV and ESV index values recommended by the guidelines for adult persons, show large differences between the lower and upper values especially for the ESV index (i.e., 12–45 mL/m^2) (20,47). The EDV, ESV and SV values obtained by means of real-time 3D-echocardiography-can also be significantly lower than those provided by MRI (48). Thus, even though there were made further progresses during the last years in the validation of 2D-echocardiography measurements and there were recently also several advancements in 3D-echocardiography techniques, there are still important challenges to be met in the future in order to achieve a better TTE-assessment of RV anatomy.

The importance of transesophageal echocardiography (TEE) for evaluation of the RV is mostly hampered by the limited movement of the transducer in the esophagus and the position of the RV in the far field (20). The most commonly selected TEE-view for the measurements of RV size and volume is a modified 4-chamber view, obtainable from the mid-esophagus in the transverse plane (i.e., imaging angle 0°). Regarding this, it must be taken into account that this view of the RV is foreshortened and can therefore not represent the real size of the ventricle (20,49). RV size measurements performed during TEE should thus be interpreted with caution. A long-axis view, which includes both inflow and outflow segments of the RV, can often be gained from transgastric longitudinal scans. Due to its limitations, in obtaining appropriate RV images, this semi-invasive diagnostic modality is less suitable for routine examinations focussed more particularly on evaluation of the RV size and geometry, especially in the presence of an appropriate TTE image quality (46). This viewpoint is also strengthened by the significant correlation between 3D-TTE- and 3D-TEE-derived RV volume measurements (50). However, TEE (especially real-time 3D-TEE) can be beneficial for the evaluation of RV size, geometry and volume in intensive care units for patients with poor TTE image quality or in the operation room for patients undergoing cardiac surgery (50).

Assessment of RV function

Assessment of RV function by echocardiography is even more challenging than the already difficult assessment of RV anatomy, and the interpretation of functional parameters can often be highly challenging.

Assessment of systolic function

The complex RV geometry does not enable reliable RV volume estimations from 2D-echocardiography-derived

images. Accordingly, the conventional calculation of the EF becomes also unreliable and, therefore, the use of 2D-echocardiography-derived RVEF estimations is no longer recommended (20,46,47,51,52).

The 3D-echocardiography is superior to standard 2D-echocardiography for estimation of RVEF and the 3D-derived RVEF showed also close correlations with the MRI-derived RVEF (20,47,53,54). However, 3D-echocardiography is technically challenging and yet not widely available (20,47). Single-beat 3D-echocardiography appeared also useful for RVEF estimation in patients with atrial fibrillation, but there is a risk of EF underestimation (55). Finally, it should not be forgotten that even the most reliable RVEF measurements do not alter the fact that because of its high afterload dependency, the RVEF is not an index of myocardial contractility (56).

Despite its aforementioned limitations, 2D-echocardiography remains highly useful for the evaluation of RV pump function because it enables assessments of other parameters like the RV fractional area-change (FAC_{RV}) and the lateral TA peak systolic excursion (TAPSE), which can reveal functional details comparable to those provided by the EF (46,57).

Both TAPSE and FAC_{RV} require no geometric assumptions and TAPSE has additionally the advantage to be measurable even in patients with reduced image quality (8,20,58). FAC_{RV} measurements revealed large interobserver and intraobserver variability and can be impaired by less optimal endocardial definition (particularly during the systole) (20,57). FAC_{RV} does not incorporate the contribution of the RVOT to ejection and can overestimate the global RV systolic function under certain clinical conditions (59). TAPSE measurements are highly angle dependent and also affected by LV function and overall heart motion (20,57). An additional limitation of TAPSE is also the gross simplification of its diagnostic value in assuming that displacement of a single wall segment could actually represent the contractile function of a complex 3D structure (20,47). Regarding this, it is important to take into consideration that TAPSE does not incorporate the contribution of the interventricular septum and that of the RVOT to the overall RV systolic performance (59,60). These limitations could explain the poor correlation between the TTE- and MRI-derived TAPSE measurements (52,61).

The major impediment to a reliable use of RVEF, FAC_{RV} and TAPSE is the fact that because of their high load dependency, they can change without any changes in the RV myocardial contractility. Thus, they will decrease with increasing PVR even if the myocardial contractility remains unchanged (8,46). TR can cause RVEF, FAC_{RV} and TAPSE changes which can become misleading for assessment of RV contractile function and can also impair the timely detection of a progressive worsening of RV myocardial contractility (i.e., reduction of responses to a given afterload) (20,46,56,62). Thus, TR can cause overestimation of RV contractile function by making the RVFW longitudinal and transversal (inward) motion easier due to the possibility of the RV ejecting a higher volume of blood during (i.e., SV_f + regurgitant flow) the systole which will correspondingly also increase the RVEF, FAC_{RV} and TAPSE values (8). Severe TR has also potentially misleading effects on the relationship between TAPSE and RVEF (i.e., worsening the correlation between them) (62).

TAPSE is also quantifiable by TEE in the midesophageal 4-chamber and deep transgastric RV view at 0° using the anatomical M-mode, where there can be a good agreement between 2D-TTE- and 2D-TEE-derived measurements (63). The deep transgastric RV long-axis view often underestimates the TAPSE (63). The RVOT fractional shortening derived from 2D-TTE measurements, which correlates well with longitudinal RV function, pulmonary arterial pressure (PAP) and RV-PA pressure gradient ($\Delta P_{RV\text{-}RA}$) can also be used for evaluation of RV systolic function (60,64,65).

Doppler-derived indices like the RV myocardial performance index (MPI_{RV}) and the rate of RV pressure rise (dp/dt), which both are not influenced by RV geometry, appeared also useful for the evaluation of RV systolic function. Although the TR-derived dp/dt ratio obtained from continuous-wave (CW) Doppler-derived measurements are easily calculable, their clinical usefulness is limited by the angle and load dependency of measurements, as well as by the lack of reliable normative data (20,47,61). RV dp/dt becomes also less accurate in the presence of severe TR because of the neglect of the inertial component of the Bernoulli equation as well as due to the increasing RA pressure (47). Indexing dp/dt to the peak systolic pressure can reduce the dependence on angle and preload (20,66). Calculations of the pulsed wave (PW) Doppler-derived RV-MPI is impaired by the impossibility to obtain the required measurements from a single cardiac cycle. Therefore, tissue Doppler imaging (TDI) is increasingly used for MPI calculation. However, the correlation between the two MPI calculation methods is poor and the normal values differ on the basis of the method chosen (47,54). Afterload dependence and the alteration of MPI values by severe TR

are other important limitations for the use of this index in the evaluation of RV myocardial contractile function (8,67). MPI also becomes unreliable in the presence of high RA pressure. (47,68). A pseudonormalization of the MPI in acute RVF induced by RV myocardial infarction has also reported (68). All these have led to the exclusion of MPI as a sole quantitative method for evaluation of RV function in current guidelines (47).

The TR duration corrected for heart rate (TRDc) considered as a surrogate for early systolic equalization of RV and RA pressure, was also found beneficial for the evaluation of RV pump function. A reduced TRDc in patients with congestive heart failure (CHF) before LVAD implantation was identified as a significant risk factor for RVF during LVAD support (69).

TDI can be particularly useful for the assessment of RV contractile function (70). An important limitation, in addition to the angle dependency of all TDI measurements, is the fixed position of the sample volume which does not enable the tracking of the surveyed area as it moves during the cardiac cycle and with respiration (60,70). Despite this, several measurements like the lateral TA peak systolic wall motion velocity (TAPS'), the RV isovolumic contraction peak velocity (IVC_V) and the RV isovolumic acceleration (IVA) were found suitable for the assessment of RV systolic function (20,71-73). An important advantage of IVA (i.e., IVC_V divided by the time-to-peak velocity), is its lower load dependency. Nevertheless, the lack of validated reference values and, even more importantly, the misleading adverse effect of TR on RV-IVC_V limit its practical usability (20,47,72). IVA measurements were also found dependent on heart rate and patient age (47). During the isovolumic contraction, RV wall motion can also be influenced by the LV contraction (e.g., traction of the RVFW at the attachment points to the LV) (58,74). In comparison with the LV, the RV wall motion evaluation by conventional echocardiography is more challenging because RV radial thickening and circumferential shortening are less marked than the longitudinal shortening and are therefore more often unable to generate a clearly visible RVFW inward movement, whereas longitudinal shortening is generally badly assessable with the naked eye.

A major limitation of wall motion (i.e., displacement and velocity) assessment by conventional echocardiography, regardless of whether the evaluated chamber is the LV or RV, is the fact that these techniques are unable to distinguish between active and passive movement of a certain myocardial segment (58,70,74). These limitations can be overcome by speckle-tracking strain imaging. Unlike wall motion, the myocardial deformation (i.e., strain) is unaffected by the motion of the entire heart and deformation analysis by strain and strain rate imaging allows not only the quantification of the myocardial deformation and deformation velocity, but also the distinction between active and passive movement of the myocardial tissue in different ventricular wall segments (46,58,70). The speckle-tracking echocardiography (STE) derived strain imaging parameters, which are also angle independent can be therefore particularly useful for the evaluation of RV contractile function (46,75). The RV global and RVFW peak systolic longitudinal strain and strain rate were found particularly beneficial for the evaluation of RV systolic function and they revealed also significant prognostic value with regard to individual risks for cardiovascular morbidity and mortality (76-78). The peak systolic longitudinal strain of the basal RVFW revealed high sensitivity and specificity for prediction of RVF after LVAD implantation (79). Strain and strain rate parameters appeared also beneficial for the evaluation of RV intraventricular dyssynchrony, a new and very promising attempt to improve the evaluation of RV dysfunction in patients with different cardiopulmonary diseases (80,81).

3D-STE appeared notably suitable for RV assessment because it allows also assessment of the relative contribution of the regional deformation heterogeneity to the global RV systolic function (80,82,83). The major limitations of STE are the high dependency on image quality, the rather modest temporal resolution and segmental reproducibility of measurements (especially for 3D-STE), as well as the unavoidable dependence of the individual measurements on the RV loading conditions (58,70). Both RV peak systolic longitudinal FW and global strain showed better correlation with MRI-derived RVEF measurements compared with conventional 2D-echocadiography-derived measurements like FAC_{RV}, TAPSE or TAPS' (61). The global peak systolic longitudinal RV strain revealed also a significant correlation with both the right heart catheterisation (RHC)-derived stroke work index (SWI_{RV}) and the 6-min walk distance (6MWD) (84,85). In LVAD candidates, the RVFW longitudinal peak systolic strain appeared also predictive for RVF after LVAD implantation but the strain data revealed a high heterogeneity (86). For a correct interpretation of STE measurements, it is essential to consider always also their load dependency (70,87). In patients with PAH RV longitudinal strain and strain rate correlate not only with the 6MWD, but also with RHC-derived hemodynamic

measurements and, after therapy, the reduction of both mean PAP (mPAP) and PVR appeared associated with a significant increase of the RV longitudinal myocardial deformation parameter values (88). Due to the relative lack of reliable normative data and their insufficient validation, STE is still not routinely used in the clinical praxis for evaluation of RV contractile function (47).

The intraventricular asynchrony of contraction quantified by calculation of a RV systolic synchronicity index (SSI_{RV}) appeared also useful for evaluation of both LV and RV systolic dysfunction in HTx and lung Tx candidates, respectively (8,88,89). The SSI_{RV} is defined by the variation coefficient of the time between the start of RV depolarization and the peak of the systolic longitudinal strain curve in six wall segments as: $SSI_{RV} = TPSL_{SD}/TPSL_{M}$, where TPSL is the time from QRS onset to the peak systolic longitudinal strain, whereas $TPSL_{M}$ and $TPSL_{SD}$ denote the mean value and the standard deviation of the measurements, respectively, in the six RV segments (8).

Assessment of diastolic function

RVF induced by pressure overload is ultimately the consequence of both systolic and diastolic RV dysfunction. Nevertheless, whereas RV systolic dysfunction has turned out to be an independent predictor of mortality in PH, diastolic dysfunction was not found to be an independent predictor of mortality in all studies (47,90). Given that the RV diastole takes place in several phases, it cannot be outlined by one single parameter and this makes the already highly challenging evaluation of RV diastolic function by echocardiography even more complicated (2). Nevertheless, certain RV diastolic parameters can be useful adjuncts in estimation of right-sided heart filling pressures, or for early detection of RV dysfunction when right-sided heart malfunction is strongly suspected but RV size and function still appear normal (47). Transtricuspid E/A flow ratio, tricuspid E/E' ratio and RA size are the best validated echocardiography-derived parameters for the evaluation of RV diastolic function (47). It should be taken into account that the impact of respiration, heart rate and preload changes on the transtricuspid flow velocities and the E/A ratio can induce misleading diastolic parameter changes (47,91).

Table 2 provides an overview of the most frequently used echocardiographic parameters for assessment of RV function, regarding their reliability and major limitations.

Quantification of functional TR

Given the deleterious impact of TR on RV size, geometry and pump function (i.e., RV volume overloading with spherical dilation and high wall tension plus reduction of the RV forward SV which reduces the CO), its significance as a major risk factor for an unfavorable outcome, as well as the negative and often also misleading impact on the echocardiographic evaluation of the RV, quantification of TR is a major goal in patients with RV dilation, particularly in those with an end-diastolic tricuspid annulus diameter >40 mm (or >21 mm/m^2). The color Doppler allows detection and semi-quantification of TR estimated by the extent of the penetration of the TR jet into the RA and inferior vena cava, as well as the measurement of the vena contracta width (92). However, the latter is not valid for multiple TR jets and small errors in the measurement of the vena contracta can result in large errors in the estimation of TR (92,93). Quantitative measurements of TR severity include the effective regurgitant orifice area (EROA), the regurgitant volume (RegVol) and regurgitant fraction (RegFr), which allow a better risk stratification (93,94). Thus, given that the RV EDV – ESV = $_{f}$SV + RegVol, the RegVol can be calculated by subtracting the $_{f}$SV from the blood volume which leaves the RV during the systole, whereas the RegFr can be calculated by dividing the RegVol by the blood volume which leaves the RV during the systole. Finally, the EROA can be calculated by dividing the RegVol by the CW Doppler-derived TR velocity-time integral (56,93). These quantitative measurements necessitate the additional use of 3D-echocardiography for the RV EDV and ESV measurements. When 3D-echocardiography is not available for assessing the RV volumes, and especially with poor 2D-TTE imagines, cardiac MRI can be very useful in both LVAD candidates and PAH patients with relevant RV dilation and TR referred for lung Tx (92-94).

Approaches and concepts for right ventricle assessment in relation to load

The high load-dependency of RV size, geometry and function confirms the necessity to consider this fundamental aspect in the interpretation of all collected data related to the evaluation of the right-sided heart. Given that no single echocardiography-derived parameter can reveal the entire picture of RV dysfunction, it is indispensable to carry out multiparametric evaluations and to adopt integrative approaches by utilizing parameter combinations which include also details about the RV loading conditions (16,95,96). During the last years, different parameter combinations related to different concepts like simple

Table 2 Reliability and major limitations of the most frequently used echocardiographic parameters for assessment of right ventricular function

Parameters	Reliability, challenges and limitations
RV ejection fraction (8,20,46,47,51,53-56,62)	• RV volume measurements necessary for EF calculations are difficult to obtain (require optimal imaging windows and image quality as well as high spatial resolution)
	• RVEF calculation using 2D-ECHO-derived RV volume measurements is not reliable and this approach is therefore not recommendable for clinical use
	• Although 3D-ECHO-derived volume measurements are more useful for RVEF calculation, the cut-off value between normal and reduced RV ejection is not fully validated, and can also be lower than those provided by MRI
	• Misleadingly higher EF values in the presence of TR and the relevant impact of RV loading conditions on the EF limit its reliability for assessment of RV systolic function
FAC_{RV} (8,20,46,57,58)	• Measurements require high spatial resolution and optimal RV endocardial definition; the inter- and intra-observer variability can be relatively high
	• Load dependency and misleading increase inducible by TR should be considered
TAPSE (8,20,46,47,52,57-63)	• Measurements are angle dependent; TEE measurements are challenging and can underestimate the RV contractile function; correlation with MRI-derived RVEF is poor
	• Influenced by overall heart motion and LV function; measurements are load dependent and misleadingly affected by TR
	• Describes only the displacement of a single wall segment
TAPS' (20,60,70)	• Measurements are angle dependent and more difficult by TEE with often underestimation of contractile function; less load dependency compared to TAPSE and FAC_{RV}
RV dp/dt (20,47,66)	• High load and angle dependency of measurements; insufficiently validated normative data; is less reliable in the presence of severe TR
TRDc (69)	• In early stages of LV failure with high afterload-induced secondary RV dysfunction, increased TRDc is a risk factor for worse outcome. By contrast, in advanced stages, after transitory "pseudonormalisation", reduced TRDc (reflecting RVF-induced increased RV filling pressure) predicts the worst outcome after LVAD implantation
MPI_{RV} (8,47,54,60,67,68)	• Can be calculated from PW and tissue Doppler measurements, but the obtained data are different
	• Only tissue Doppler enables the taking of all the necessary measurements from one cardiac cycle
	• A pseudo-normalization of the MPI_{RV} in advanced RVF the adverse impact of afterload, as well as RV hypertrophy and severe TR can be misleading
IVC_V and IVA (20,47,71-73)	• The lack of reliable reference values, the angle dependency of measurements, the impact of heart rate and simultaneous LV contraction on measurements and the negative impact of TR makes the interpretation of these parameters often challenging. By contrast, their only moderate load dependency can be a great advantage
RVSL and RVSrL (46,58,70,75-78)	• Measurements require good image quality and the relatively poor temporal resolution as well as the low segmental reproducibility of measurements (particularly with the use the 3D-speckle-tracking technique) should be taken into consideration.
	• In contrast to the angle independent speckle-tracking derived data, the TDI-derived measurements are angle dependent
	• The load dependency of measurements (particularly that of the strain parameters) must be taken into account during the interpretation of the measurements
E, A, E/A, E/E' (47,90,91)	• Respiration, heart rate and preload changes, as well as relevant TR can induce misleading changes in these diastolic parameters

RV, right ventricle; EF, ejection fraction; MRI, magnetic resonance imaging; TR, tricuspid regurgitation; FAC_{RV}, RV fractional area change; TAPSE, lateral tricuspid annulus peak systolic excursion; TEE, transesophageal echocardiography; LV, left ventricle; TAPS', lateral tricuspid annulus peak systolic wall motion velocity; dp/dt, rate of RV pressure rise; TRDc, TR flow duration corrected for heart rate; RVF, RV failure; LVAD, LV assist device; MPIRV, RV myocardial performance index; PW, pulsed wave; IVCV, RV isovolumic contraction peak velocity; IVA, isovolumic acceleration; RVSL, RV longitudinal strain; RVSrL, RV longitudinal strain rate; TDI, tissue Doppler imaging.

ratio of function and load, RV-PA coupling, or indices for assessing the RV ability to face abnormally high PVR have been proposed for evaluation of the RV adaptability to overloading (5,8,96). However, optimal integrative approaches necessitate both echocardiography-derived and RHC-derived variables, because most of the tested approaches based only on echocardiographic parameters appeared limited due to the lack of more precise hemodynamic data. Accordingly, the RV stroke-work index (SWI_{RV}), calculated from RHC-derived measurements, was found more reliable than several echocardiographic parameters which are currently used for the evaluation of the RV in end-stage CHF (97,98). There was also found only a weak correlation between the RHC-derived and the echocardiography-derived SWIRV values (97). Meanwhile, two simplified and easily calculable composite echocardiographic parameters were suggested as surrogates for the SWI_{RV} (99,100). One of them, the "RV contraction-pressure index" (RVCPI), which is calculated as RVCPI = TAPSE × ΔP_{RV-RA}, where ΔP_{RV-RA} is the pressure gradient between RV and RA, showed a strong correlation with the RHC-derived SWI_{RV} and also a high sensitivity and specificity to predict a reduced SWI_{RV} (99,101,102). In a prospective study on patients with acute decompensation of advanced CHF, multivariate analyses revealed the presence of a low RVCPI as the best predictor of outcome, whereas neither TAPSE or FAC_{RV}, nor TAPSE/systolic PAP or FAC_{RV}/systolic PAP revealed significant predictive values (101). The usefulness of the RVCPI as an independent predictor of short-term postoperative patient outcome (including RVF) after LVAD implantation was confirmed also more recently (102). The other echocardiography-derived surrogate for the RHC-derived SWI_{RV} referred to as "RV stroke work" (RVSW), also revealed a good correlation with the RHC-derived SWI_{RV} (100). It incorporates the SV and load and is calculated as: RVSW = 4 × [TR jet peak velocity]^2 × [pulmonary valve area × VTI], where VTI is the velocity-time integral of the systolic transpulmonary jet (100).

During the last decade, certain echocardiography-derived composite indices which integrate either the longitudinal ventricular wall displacement and afterload (i.e., TAPSE/systolic PAP and TAPSE/PVR) or the velocity of myocardial shortening and load (e.g., the "afterload-corrected peak systolic longitudinal strain rate") had also proved to be suited for the evaluation of RV contractile function (5,8,103-106). The TAPSE/systolic PAP ratio is an easier strategy to assess RV contraction by plotting longitudinal myocardial shortening *vs.* the force generated for overpowering the increased load (103-106). In essence, TAPSE/systolic PAP facilitates the valuation of RV contractile ability, which in turn can be helpful in both estimation of prognosis and therapeutic decision making. Based on its correlation with the invasively calculated RV systolic elastance/arterial elastance ratio (P<0001), TAPSE/systolic PAP was also suggested as a non-invasive index of RV-PA coupling (106). Several larger clinical trials showed a high reproducibility of the necessary measurements and this index was also identified as a powerful predictor of mortality in patients with HF due to primary impaired LV function, as well as in patients with advanced PAH (69,96). However, the significant predictive value for mortality in patients with severe congestive HF could not be confirmed in all studies (101). Another simple echocardiography-derived composite variable which was suggested as a potentially useful index of RV-PA coupling is the RV ejection efficiency (RVEe), defined as RVEe = TAPSE/echoPVR (104). Using TAPSE as a surrogate for RV ejection and the echoPVR (i.e., PVR = TR peak velocity/RVOT velocity-time integral) as surrogate for the RHC-derived PVR, the RVEe becomes easily calculable. The reliability of PVR measurement by echocardiography was for a long period of time a controversial issue (47,104,107). However, evaluations of data from five validation studies yielded a good correlation between RHC-derived and the echocardiography-derived PVR measurements (108). Thus, the determination of the echocardiography-derived RVEe might be helpful for the assessment of RV systolic function. However, additional studies are warranted to establish whether the RVEe index can be really useful for RV evaluation. A limitation of this index is its decreasing reliability with the increase of the TR in patients with high afterload-induced severe RV dilation. It is well established that severe TR is a significant confounding factor that can affect the use of TAPSE for assessing RV function (20,46,56,62).

The SV/RV ESV ratio (SV/RVESV), was also suggested as a potentially useful surrogate for the RV-PA coupling which facilitates the evaluation of myocardial contractility corrected for afterload (109). The incorrect inherent assumptions that the relationship between the RV end-systolic pressure and RV endsystolic volume is linear and crosses the origin and that also for the RV, Ees coincides with Emax can be a potential limitation of the SV/RVESV ratio which may reduce its reliability (109). An additional impediment is the unreliable measurement of RV volumes with 2D-echocardiography. For this reason, it was suggested

to use the RV area change/RV end-systolic area as a surrogate for RV-PA coupling, an approach whose potential usefulness as a prognostic marker in patients with severe PAH was already confirmed by one study (96).

The afterload-corrected peak global systolic longitudinal strain rate (SRl), which is calculated by multiplying the measured global RV systolic SRl value (also known under the abbreviation PSSrL) with the $\Delta P_{RV\text{-}RA}$ and, thereby, reflects the linkage between RV myocardial shortening velocity and RV load is a well reproducible and easily measurable combined parameter for evaluation of the RV contractile function in relation to load (5,8). Due to the fact that shortening-velocity is load dependent, the peak global systolic SRl will decrease simultaneously with the increase of RV systolic pressure. Under these circumstances, as long as the RV contractile function remains unchanged, due to the increase of $\Delta P_{RV\text{-}RA}$, the RV load-corrected peak global systolic SRl (i.e., SRl • $\Delta P_{RV\text{-}RA}$) remains relatively stable. As soon as the afterload increase overwhelms increase the ability of the RV to respond correspondingly by further increase of the systolic pressure (i.e., afterload mismatch), in addition to the SRl reduction there will also be a $\Delta P_{RV\text{-}RA}$ reduction caused initially by the increase of RA pressure, even before the RV systolic pressure will finally also become lower according to the degree of RV contractility impairment induced by the consequences of overloading. The load-corrected peak global systolic SRl is therefore more reliable for the assessment of RV contractile function than the peak global systolic SRl alone (5,8).

The 3D-STE-derived volume measurements in combination with the RHC-derived PAP were also used to evaluate the relationship between RV remodeling and afterload (110). Regression analysis between systolic PAP and RV EDV-index was found to be able to distinguish between adapted, adapted-remodeled and adverse remodeled RV (110).

A different approach for the evaluation of RV adaption to high afterload is provided by the "RV load-adaptation index" (5,8). In principle, this composite echocardiography-derived index is based on the relationship between RV dilation and the RV loading conditions, given the fact that in patients with similar cardiac index and resistance to the blood flow in the pulmonary circulation, less RV dilation indicates better adaptation to high afterload. Using for the calculation of the RV load-adaptation index the easy and reliably measurable TR velocity-time integral (VTI_{TR}) as a surrogate of the hemodynamic load and the end-diastolic RV area (A_{ED}) as an alternative to the not reliably measurable RV EDV for obtaining a reliable RV size-geometry index, allows the obtainment of a highly reproducible dimensionless index (5,8,95):

$$RV\ load\text{-}adaptation\ index = \frac{VTI_{TR}}{A_{ED} / L_{ED}} = \frac{VTI_{TR}\,(cm) \cdot L_{ED}\,(cm)}{A_{ED}\,(cm^2)} \quad [1]$$

The use of the VTI_{TR} as a surrogate of the RV hemodynamic load is reasonable and possible because, particularly in patients with relevant TR, the $\Delta P_{RV\text{-}RA}$, which is computed from the mean velocity of the TR jet, reflects in a more optimal way the RV loading conditions than the estimated systolic PAP (5,8). The use of the VTI_{TR} is more beneficial because it includes also the duration of the after-loading during the RV systole (8,95). Inclusion of the end-diastolic and not the end-systolic RV area and long-axis measurements into the load-adaptation index calculation formula is more appropriate for the purpose because RV dilation is more reliably quantifiable in the end-diastole, especially in patients with relevant TR (TR leads to underestimation of the RV dilation in the end-systolic phase) (8,95). The utilization of A_{ED} instead of EDV is justified by the close correlation between the echocardiography-derived RV-A_{ED} and the MRI-derived RV-EDV (111). Thus, a small RV area relative to long-axis length (i.e., no dilation) in the presence of an increased VTI_{TR} (i.e., high RV systolic pressure accompanied by a relatively low RA pressure) generates a high load-adaptation index which indicates a good adaptability of the RV to pressure overloading (i.e., RV ability to increase the systolic pressure without relevant cavity dilation and without increase of RA pressure) indicating the existence of an optimal RV contractile function and the ability of the RV to improve its pump function after reduction of pressure overloading. A large area relative to long-axis length (i.e., spherical dilation) in the presence of a relatively low VTI_{TR} generates a low load-adaptation index which suggests a poor adaptation to load (i.e., disproportionally excessive RV dilation associated with reduced RV systolic function) which suggests an impaired myocardial contractility. In healthy persons and patients with PH without impaired RV contractile function, the RV load-adaptation index values are ≥18. In patients with RV dysfunction, load-adaptation index values <15 indicate a reduced RV adaptability to load which can be insufficient to prevent RVF even after normalization of PVR(5,95,96,112).

Recently, the RV global work efficiency defined as RV global constructive work (i.e., the work contributing to the shortening of the cardiac myocytes during systole and their lengthening during the isovolumic relaxation)

divided by the sum of RV global constructive work and RV global wasted work (i.e., the work contributing to the lengthening of the cardiac myocytes during systole and the shortening during isovolumic relaxation), a more complex echocardiography-derived parameter combination for assessing the RV in relation to its loading conditions was found useful for predicting the risk of early right HF (RHF) after LVAD surgery (113). In that small study, the predictive value of the RV global work efficiency was superior to that of both the TAPSE/systolic PAP (sPAP) and the RVFW longitudinal strain/sPAP ratio.

Clinical usefulness of right ventricle evaluation in relation to load

Several studies using variable methodology revealed significant correlations between RV systolic function and patient outcome across a large spectrum of diseases (5,8,51,111,112,114-117). Despite this, although the relevancy of RV function in the prognostic assessment and clinical management and of numerous cardiovascular diseases is irrefutable, it is not easy to include RV functional alterations into therapeutic decision-making. This, however, is unavoidable particularly before HTx or LVAD implantation, where the assessment of the RV in connection with its loading conditions has proved to be particularly useful in accurate decision-making, as well as for timing of lung Tx-listing for patients with refractory advanced precapillary PH (95,118). Given the limitations of echocardiography in the hemodynamic evaluation of patients with HF, as well as the limitations of RHC in the evaluation of cardiac structural and functional abnormalities, neither echocardiography, nor RHC allows alone a reliable clinical management of these patients. However, the combined use of echocardiography and RHC has proved to be a crucial tool for the evaluation of HF patients and therapeutic decision-making.

Given the particular importance of a reliable quantification of both RV dilation and TR severity for the clinical decision-making in LVAD candidates or patients with pharmacological therapy refractory severe PAH, in some cases, it will be reasonable to use cardiac magnetic resonance (CMR) measurements which are more reliable than those provided from echocardiography (119,120).

Usefulness for evaluation of patients referred for ventricular assist device implantation

Both ventricles are usually affected in advanced HF, even if it originated from a left-sided heart disease. Even though an LVAD provides better survival and quality of life than a BiVAD, one must also consider that RVF can arise in almost 25% of patients supported by an LVAD (121,122). Due to its close association with high postoperative morbidity (e.g., renal, hepatic or multiorgan failure) and mortality [even if LVAD placement is later followed by additional right VAD (RVAD) insertion], the presence of a severe RVF in LVAD recipients must be avoided (121,122). Therefore, both patients who require a durable BiVAD support and those who need only a temporary RVAD in addition to the LVAD must be detected already pre-operatively or not later than intraoperatively (95,123). In the meantime, it has become obvious that echocardiography can be a cornerstone for the timely identification of those patients.

Patients with further worsening of RV function after LVAD implantation, revealed already before LVAD implantation more serious alterations of echocardiographic parameters reflecting the RA and RV size, geometry and function (69,86,98,124-136). Particularly the RV end-diastolic diameters and short/long axis ratio (S/L_{ED}), the RV/LV diameter-ratio, as well as the FAC_{RV}, TAPSE, TAPS', peak systolic global longitudinal strain and strain rate, RA diameter, TRDc, and TR severity were found to be beneficial parameters for the assessment of the right-sided heart before VAD implantation (8,95,126,134-143). In LVAD candidates, S/L_{ED} >0.57, RV/LV diameter ratio ≥0.75, FAC_{RV} <30%, TAPS' <8 cm/s, TR >2nd degree, $\Delta P_{RV\text{-}RA}$ <35 mmHg, peak systolic global longitudinal strain and strain rate <–9.6% and <0.6/s, respectively, as well as LA volume-index <38 mL/m² were identified by univariate analysis as relevant risk factors for RVF after LVAD implantation. Preoperative RV/LV diameter-ratio ≥0.75, TA dilation and TR ≥ moderate-to-severe, were identified as significant risk factors for RVF after LVAD implantation, also by multivariate analysis (8,27,131-133,136,138,140-146). Nevertheless, these preoperative anatomical and functional RV alterations could not be found in all studies to be significant risk factors for RVF during LVAD support (51,130,142). This could be partially explainable also by the remarkable disparities between individual clinical units regarding the criteria used for both defining RVF and the selection of patients and devices for ventricular support (51,86). *Table 3* provides an overview of the risk discrimination capacity of echocardiography for preoperative prediction of RHF after LVAD implantation.

Nearly all of the echocardiography-derived parameters whose pathological alterations were identified as significant

Table 3 Risk discrimination capacity of echocardiography for preoperative prediction of right-sided heart failure during left ventricular long-term mechanical support

Variables	Cut-off values	Prognostic performance for RV failure during LVAD support (%)			
		Sensitivity	Specificity	PPV	NPV
RV peak systolic SRI, /s (5)	0.6	80	98	92	95
RV load-corrected peak systolic SRI, mmHg/s (5)	24	89	96	97	87
RV load adaptation index (5)	14	91	95	83	97
RV echocardiographic score* (143)	–	87	87	91	81
Left-sided heart echo-score† (131)	≥3	89	80	80	91
ΔP_{RV-RA}, mmHg (5)	35	84	93	96	76
RV global PLS (4c view) (142)	–9.7%	89	78	84	84
RV PLS_{basal} (79)	–	86	95	67	95
TAPS', cm/s (5)	8	84	90	95	70
RV global work efficiency (113)	77%	100	82	60	100
TAPSE/longitudinal RVEDD (144)	17.1%	78	68	67	77
RVFW peak systolic LS§					
(98)	–19%	86	95	91	82
(133)	–9.6%	68	76	76	68
RV global peak systolic LS§ (139)	–14.4%	83	66	92	51
TAPSE, mm§					
(130)	<7.5	46	91	85	67
(98)		Not predictive for RV failure before LVAD implantation			
RV-S/L_{ED} (5)	0.57	84	74	94	46
TTE score [points (p)]‡,§ (132)	≥5	63	78	75	64
RA longitudinal strain (135)	<10.5%	94	65	33	98
Tricuspid annulus diameter, mm$,§ (146)	41	73	75	29	90
RV E/E'§ (139)	10.2	83	57	44	90

*, the components of this score are: LV diameter, RV global longitudinal strain, TR ≥ moderate, pulmonary acceleration time, pulmonary acceleration-to-ejection time ratio. †, the components of this score are: the components of this score are: LV end-diastolic diameter, left atrial/LV end-diastolic diameter ratio, LV ejection fraction. §, assessed by multivariate analysis. ‡, the components of this score are: RV fractional area change, estimated RA pressure, left atrial volume index. $, this study is focused on prediction of late post-LVAD (>30 days) RVF. RV, right ventricle; LV, left ventricle; LVAD, LV assist device; PPV, positive predictive value; NPV, negative predictive value; SRI, longitudinal strain rate; RA, right atrium; P_{RV-RA}, pressure gradient between the RV and RA; PLS, peak longitudinal strain; TAPS', lateral tricuspid annulus peak systolic wall motion velocity; TAPSE, lateral tricuspid annulus peak systolic excursion; RVEDD, RV end-diastolic diameter; RVFW, RV free wall; LS, longitudinal strain; $S/L_{ED,}$ end-diastolic short/long axis ratio; TTE, transthoracic echocardiography; E/E', early diastolic transtricuspid flow/lateral tricuspid annulus early diastolic peak velocity ratio; RVF, RV failure.

risk factors for RVF after LVAD implantation (particularly FAC_{RV} and MPI) appeared alone not able to predict preoperatively the RV function during LVAD support (51,130). Until now, only TAPS' and both peak systolic global longitudinal strain and strain rate revealed alone significant predictive values for post-operative RV function in LVAD candidates (5,86,133,147,148). For decision in favor or against the necessity of a BiVAD support, it appears to be much more reliable to use composite variables which include, in addition to details on RV geometry and function,

also parameters which reflect the RV loading conditions (5,8,148,149). Thus, several echocardiographic parameters became more predictive for post-LVAD RVF if they were utilized in combination, either as part of a scoring-system or as part of a composite index variable (5,126,131,132). At certain cut-off values, different echocardiography-derived composite variables and scoring systems yield preoperatively positive and negative predictive values for post-LVAD RVF which ranged between 75–97% and 64–97%, respectively (*Table 3*). Up to now, the highest predictive values (≥80%) for both RVF and freedom from RVF after LVAD implantation were found for three STE-derived parameters (i.e., the peak systolic global longitudinal strain and strain rate, as well as the RVFW longitudinal strain), two composite echocardiography-derived variables and two echocardiographic scores (*Table 3*) (5,98,131,133,142,143). So far, for different objective reasons, the clinical value of different echocardiographic parameters for pre-implant prediction of post-implant RV function in LVAD candidates were more often assessed by univariate analysis. However, as shown in *Table 3*, even studies which used multivariate analysis can reveal different predictive values for the same echocardiographic parameter (98,133). Based on the available evidence, currently there is not possible to establish a hierarchy of echocardiography-derived parameters based on their ability for pre-implant prediction of post-implant RV function in LVAD candidates (86,150).

Role in evaluation of lung transplant candidates with precapillary PH

RVF induced by pressure overload is the leading cause of mortality among patients with severe PAH and chronic thromboembolic PH (CTEPH), and the mortality rate of PAH patients with acute RHF can reach 40% (151-155). With the continuous prolongation of waiting times for Tx, early prediction of irreversible RVF in candidates for lung Tx is of crucial relevance for optimal timing of listing procedures, and the search for reliable prognostic predictors remains further a major goal (156-158).

Prognosis of the risk for life-threatening cardio-respiratory failure in PAH patients is primarily based on RHC-derived hemodynamic measurements which, being invasive, are less frequently repeatable and not always feasible for early baseline stratification of PAH patients (156-160). In addition, hemodynamic measurements alone are often insufficient for a reliable prediction of impending life-threatening deterioration RV function, because of the lack of direct information about the impact of the pressure overloading on the RV size and geometry. Echocardiography can provide that missing information, and certain parameters like FAC_{RV}, TAPSE and TAPS' revealed also a strong correlation with MRI-derived RVEF (161,162). In patients with PAH and CTEPH, univariate analysis revealed that pericardial effusion (PE), increased RA area-index, RV end-diastolic diameter, RV EDA- and RV ESA-index, RV end-systolic remodeling index (RVESRi = end-systolic lateral length/septal high), RV diastolic and systolic eccentricity index and MPI_{RV}, as well as reduced TAPSE and systolic peak IVCv at the TA, reduced RV longitudinal strain and strain rate, severe TR and RV dyssynchrony, can be significant risk factors for mortality (8,96,163-173). However, multivariate analyses have identified only the PE, the severe TR, the increased RVESRi and RA size, the increased MPI_{RV}, as well as the reduced systolic peak IVCv and reduced peak systolic longitudinal strain rate (PSSrL) as significant risk factors for death in those patients (96,165,169).

Nevertheless, those parameters could not be identified in all studies as significant risk factors for mortality without urgent Tx and actually no single echocardiography-derived parameter except the presence of PE has univocally proved to be a reliable prognostic indicator (8,159). Given that the PE is not an early indicator of RVF it can reasonably be concluded that timely identification of patients at imminent risk for short-term development of RVF by echocardiography in order to improve Tx-listing procedures is challenging and there is no single echocardiography-derived parameter which could be alone sufficiently reliable for a timely prediction of irreversible RVF in the course of advanced precapillary PH.

Several studies revealed in patients with PAH and CTEPH already before the first RVF episode significant differences in certain echocardiography-derived parameters like end-diastolic RV diameter, S/L_{RV}, TAPSE, TAPS', load-corrected peak global systolic SRl, RV systolic longitudinal synchronicity index, TR severity and $\Delta P_{RV\text{-}RA}$ between those who later developed RVF and those who remained free from RVF (8,76,173-177). TAPSE and peak systolic global SRl were found by univariate analysis to be relevant risk factors for RVF and the load-corrected PSSrL (i.e. peak global systolic SRl) was identified as a significant risk-factor for RVF also by multivariate analysis (8). Nevertheless, the predictive values of all these variables for occurrence of RVF has proved to be only modest due to their rather modest specificity ranging only between 56.5% and 73.9% (8,173). In PAH, RVFW longitudinal strain values below –12.5%

Table 4 Risk discrimination capacity of echocardiography for prediction of imminent worsening of right ventricular function in potential lung transplant candidates with pre-capillary pulmonary hypertension

Variables	Cut-off values	Prediction (%) of RV worsening			
		Sensitivity	Specificity	PPV	NPV
RV load adaptation index (8)	35	94	74	90	85
	Reduction with ≥20%*	96	78	91	90
RV load-corrected peak global systolic SRI, mmHg/s (8)	45	91	70	88	76
RV peak GLS (174)	–16.6%**	79	56	48	84
	–12.7%†	77	76	37	95
RV peak GLS (175)	–13.4%‡	73	91	68	77
RV peak GLS (173)	–14.0%$	100	55	100	65
RV synchronicity index, ms◊ (177)	37.6§	84	80	44	96
FAC_{RV} (175)	25.7%	87	83	65	89
TAPSE, cm (174)	1.7**	46	68	44	69
	1.4†	40	87	36	88
EDD_{RV}, S/L_{ED}, ΔP_{RV-RA}, TR, TAPS', SSI_{RV} (8)	Rather moderate predictive values for development of RVF during the next 1 to 3 years, with PPVs between 60–68%, and NPVs between 81–88%				
EDA_{RV}, RA_{area}, TAPSE, FAC_{RV}, PAPs, RVGLS (176)	These parameters collected before lung transplantation appeared in this study unable to predict post-transplant outcome				

*, reduction of >20% of the baseline (initial) value. **, major worsening. †, 1-year mortality. ‡, major worsening ± death. $, transplant-free survival. §, mortality after diagnosis during a mean follow-up of 42±15 months. ◊, index calculated from speckle-tracking strain images using the apical four-chamber view. RV, right ventricle; PPV, positive predictive value; NPV, negative predictive value; SRI, longitudinal strain rate; GLS, global longitudinal strain; FAC_{RV}, right ventricular fractional area change; TAPSE, lateral tricuspid annulus peak systolic excursion; EDD_{RV}, RV end-diastolic diameter; $S/L_{ED,}$ end-diastolic short/long axis ratio; ΔP_{RV-RA}, pressure gradient between the RV and RA; TR, tricuspid regurgitation; TAPS', lateral tricuspid annulus peak systolic wall motion velocity; SSI_{RV}, RV systolic synchronicity index; RVF, RV failure; EDA_{RV}, right ventricular end-diastolic area; PAPs, systolic pulmonary arterial pressure.

showed only sensitivity and specificity values between 71% and 67%, respectively, for the emergence of clinically relevant RHF, and even lower values (only 54% and 64%, respectively) for occurrence of all cardiovascular adverse events (death included) (75). Standard functional parameters like TAPSE and FAC_{RV} also showed only modest sensitivity for prediction of the MRI-derived RVEF worsening (162). It was also observed that, with progression of RV dysfunction, TAPSE reduction reaches a limit after which it does not further decrease, even with further aggravation of RV dysfunction (178). This could be at least partly related to the worsening of secondary TR which facilitates the longitudinal RV wall motion correspondingly to the higher blood volume which can leave the RV during the systole and can thus also impede prevent a further reduction of TAPSE during an ongoing reduction of RV pump function. RV intraventricular dyssynchrony quantified from 2D-STE-derived longitudinal strain measurements in 6 ventricular wall segments appeared also independently predictive for event-free survival in patients with PH (179).

The load-adaptation index and the load-corrected PSSrL, were found particularly suited for RV evaluation and appeared also significantly predictive for development of RVF in the presence of PAH and CTEPH. The load-corrected PSSrL and the RV load-adaptation index showed positive and negative predictive values between 88–91% and 76–90%, respectively, for the development of RVF during the subsequent 2 months (*Table 4*) (8). The 20% cut-off value for the RV load adaptation reduction, before the first appearance of any signs or symptoms of RVF, allows the prediction of RVF development and RHF-free outcome during the subsequent 12 months with 91% and 90% probability, respectively (8). In PAH patients, the RV load-adaptation index values are usually >25 (i.e., within or above the normal range for healthy people), even in the presence of

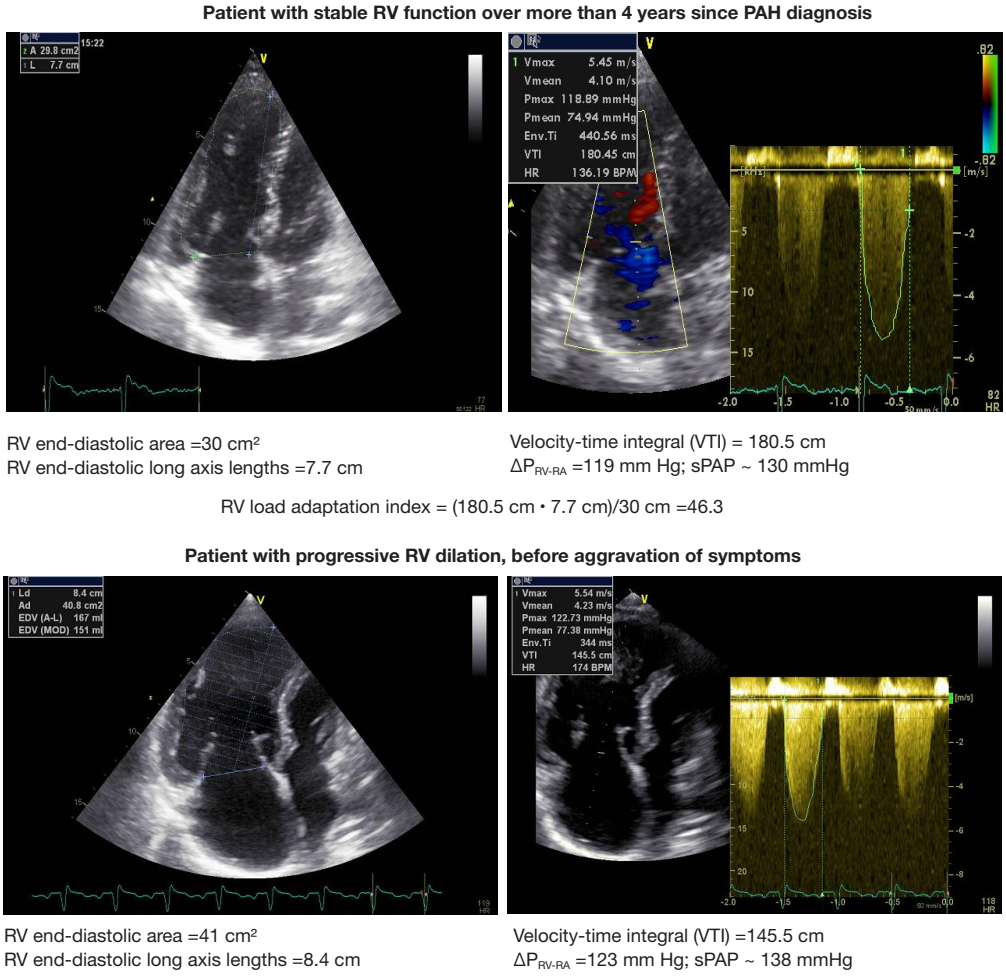

Figure 3 Different right ventricular load adaptation in 2 patients with massive pulmonary arterial hypertension and nearly identical pulmonary arterial pressure. Given that in both patients the RV was able to develop a systolic and mean PAP of more than 130 and 74 mmHg, respectively, indicates that their RV systolic function is far better than that of healthy persons. However, the progressive RV dilation in the second patient indicates the existence of an impending risk of RV-pulmonary arterial uncoupling with rapid reduction of cardiac output, which arguments against a delay of the recommended lung transplantation. RV, right ventricle; PAH, pulmonary arterial hypertension; ΔP_{RV-RA}, pressure gradient between the RV and right atrium; sPAP, systolic pulmonary arterial pressure.

RVF, indicating that in most of all those patients, the trigger of RVF is the excessive pressure overload and not an impaired RV contractility (8). This explains the reverse remodeling with relevant improvement (up to normalization) of RV pump function after lung transplantation in the majority of patients with pre-capillary PH. *Figure 3* shows echocardiographic images of 2 PAH patients with nearly identical extremely high PAP values, which indicate a supranormal systolic function. However, the risk of a RV functional decompensation of these patients is different because the RV load adaptation index turned out to be 64% lower in the patient with RV dilation when compared to that of the patient without RV dilation.

Usefulness in the management of COVID-19-related ARDS

Given the high prevalence of extensive pulmonary thrombotic microangiopathy associated with severe ventilation-perfusion mismatch, increased pulmonary vascular resistance and frequent afterload-induced acute RVF, which were identified as distinct features of severe COVID-19-related ARDS (especially in infections caused by the Delta/B.1.617.2 variant), it is not surprising that

RV dilation and dysfunction were found independently associated with a significant increase in mortality risk and that RVF was often identified as the leading cause of death attributed to COVID-19 (9-12,180-183). Especially during the 2nd pandemic wave, between 80–100% of the lungs examined at autopsies revealed platelet-fibrin thrombi in the small pulmonary vessels, and microangiopathy with widespread thrombosis were found up to 9 times more frequent than in the lungs from patients who died from influenza (184-189). In one study, intravascular pulmonary microthrombosis was detected during autopsy in the lungs of all persons who died from COVID-19, and in all of them, the cause of death was related to the pulmonary lesions (189). These observations indicate that in COVID-19-related severe ARDS, with severe RV afterload mismatch associated with relevant RV output reduction which will be further aggravated by RV dilation-related rapidly increasing TR, any attempts to improve the blood oxygenation by optimizing the mechanical ventilation and even the use of veno-venous-ECMO may become insufficient, as long as the blood circulation in the small pulmonary vessels is severely impaired (10,181). It is proven that the increase in pulmonary arterial resistance and pressure can be a factor 4 to 5 compared with only about 50% in the systemic circulation (183). However, this adaptive response can be attained only during chronic pressure overloading and not without the development of a pronounced RV hypertrophy. When faced with an acute increase in afterload, the normal RV is able to increase peak systolic pressure up to maximum ~60 mmHg associated with RV dilation, before RV contractile failure and systemic hypotension ensue (190). This explains the observations that the acute cardiorespiratory decompensation in severe SARS-CoV-2 pulmonary infection occurs typically only about one week after initial symptom onset and that the simultaneous detection of RV dilation and dysfunction by TTE performed on median day 6 after admission to intensive care units appeared independently associated with in-hospital mortality (191,192). Thus, the early appearance of RV dilation in hospitalized patients with SARS-CoV-2 pneumonia should be considered as a potentially important indication for an acute increase of the RV afterload even in the presence of a rather moderate increase of the systolic PAP, when compared to the much higher PAP values in relative stable patients with chronic PAH. Given that the life-threatening SARS-CoV-2 related widespread small vessel thrombosis occurs typically only several days after the onset of clinical symptoms, the monitoring of RV size and geometry appears necessary in all patients with moderate RV dilation especially in those with systolic PAP ≥40 mmHg. *Figure 4* provides an overview on the impact of heart-lung interactions on the development and progression of potentially life-threatening RV dysfunction during SARS-CoV-2 pulmonary infection in patients without direct damage to the myocardium.

Early detection of progressive hemodynamic overloading of the RV in the course of a severe SARS-CoV-2 pulmonary infection can facilitate the selection of the most appropriate management (including the requirement of veno-arterial ECMO or a combined respiratory and circulatory support), which can be decisive for their survival (10,181,193). Being the most frequently involved side of the heart in COVID-19 and because RV dilatation and dysfunction were identified as the most striking echocardiography abnormalities in hospitalized patients with SARS-CoV-2 infection, the right-sided heart deserves particular consideration in those patients. Echocardiography can help anticipate an aggravation of the patient's clinical condition. Timely detection and severity evaluation of right heart over-loading plus prediction of RVF are key issues to ensure the best possible care of hospitalized patients. Regarding this, close surveillance of RV and RA size and geometry, search for TR and assessment of its progress, as well as monitoring of the SV and the $\Delta P_{RV\text{-}RA}$ are essential (10). Evaluation of RV-PA coupling using the FAC_{RV}/RV systolic pressure, plus assessment of RV adaptability to pressure overloading using the RV load-adaptation index could also allow prognostic statements to be made (10). In a large multicentre prospective study on COVID-19 patients requiring invasive mechanical ventilation, abnormal RV-free wall longitudinal strain (FWLS) (below –20%) was found independently associated with 30-day mortality (170). This study supports the importance of early identification of RV dilation and dysfunction by echocardiography for timely recognition of patients at high risk for life-threatening cardiocirculatory complications, thus avoiding delays in the implementation of appropriate therapeutic measures (194).

Because the different waves of infection were mainly associated with one or more SARS-CoV-2 "variants of concern" (VOC) with different pathogenicity, it appears obvious that the pathogenicity of the dominant VOC in an infection wave can have important impacts on the outcomes of patients with severe COVID-19. Although currently both the incidence and the severity of pulmonary SARS-CoV-2 infections are in regression, the role of heart-lung interactions in the emergence and progression of potentially

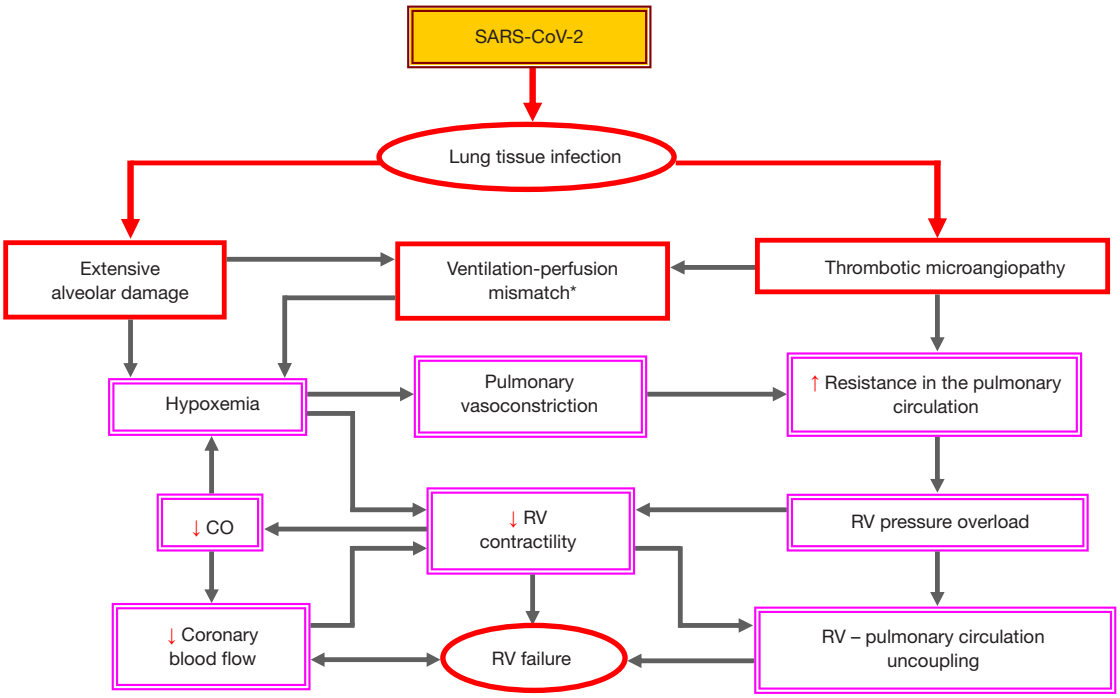

Figure 4 Key pathophysiological mechanisms involved in the occurrence and progression of severe secondary RV failure during SARS-CoV-2 pulmonary infection associated with widespread thrombotic microangiopathy. Red bold arrows show the major direct damaging effects of the virus on the pulmonary tissue. ↓ and ↑ in the boxes stand for reduced and increased, respectively. *, coexistence of shunt and dead space ventilation. SARS-CoV-2, severe acute respiratory syndrome coronavirus; RV, right ventricle; CO, cardiac output.

life-threatening RV dysfunction during SARS-CoV-2 pulmonary infection should continue to be considered because a renewed appearance of more pathogenic VOCs cannot be ruled out.

Conclusions

During the last decades, simultaneously with the progresses made in the diagnosis and therapy of PH and especially since implantation of long-term ventricular assist devices has become a widely recognized life-saving treatment for end-stage refractory HF, focused assessment of RV size, geometry and function has emerged as a crucial part of cardiac evaluation which includes echocardiography as an indispensable cornerstone. Nevertheless, it is important to note that due to the relevant anatomical and functional particularities of both the normal and the pathologically altered RV its evaluation is not simply possible by extrapolating data and vast experience gained from the echocardiographic evaluation of the LV. Particularly challenging can be the correct interpretation of the echocardiography-derived measurements regarding to their diagnostic and prognostic relevance. There are several well-established limitations in the assessment of the RV by echocardiography and in the integrative interpretation of collected measurements which should always be considered.

The high load-dependency of RV size, geometry and function suggests the need to consider this fundamental aspect in the interpretation of the collected data related to the evaluation of the right-sided heart. Because not a single echocardiographic parameter can reveal alone the entire highly complex clinical picture of RV dysfunction it is mandatory to perform multiparametric evaluations and to apply integrative approaches using parameter combinations which include also information about the RV hemodynamic loading conditions. At certain cut-off values different echocardiography-derived composite variables and scoring-systems revealed positive and negative predictive values for post-LVAD RVF ranging between 75–97% and 64–97%, respectively. Certain composite echocardiography-derived variables have proved to be able to facilitate timely decision-making for LVAD implantation before RV dysfunction and/

or end-organ damage become irreversible.

In patients with advanced precapillary PH, several echo-derived parameters which were identified as significant risk factors for RVF (e.g., TAPSE and RVFW longitudinal strain) revealed, nevertheless, only modest predictive values for development of RVF. Only composite echo-derived parameters which included also parameters related to the loading conditions appeared so far sufficiently predictive for imminent development of RVF, and, thereby also useful for clinical decision-making.

Theoretically, the major questions which need to be answered in the presence of RV dysfunction associated with high resistance to blood flow in the pulmonary circulation are related to the relative contribution of hemodynamic load, pathological (maladaptive) RV remodeling and impaired myocardial contractility, as well as to the potential reversibility of RV dysfunction. However, currently many of those questions are often not reliably answerable even by multimodality approaches and multiparametric evaluations. Regarding the contribution of echocardiography to improve the clinical decision-making, it appears meaningful to take also the RV adaptability to increased hemodynamic afterload into account.

Acknowledgments

Funding: None.

Footnote

Peer Review File: Available at https://cdt.amegroups.com/article/view/10.21037/cdt-23-380/prf

Conflicts of Interest: The author has completed the ICMJE uniform disclosure form (available at https://cdt.amegroups.com/article/view/10.21037/cdt-23-380/coif). The author has no conflicts of interest to declare.

Ethical Statement: The author is accountable for all aspects of the work in ensuring that questions related to the accuracy or integrity of any part of the work are appropriately investigated and resolved.

References

1. Bernardo RJ, Haddad F, Couture EJ, et al. Mechanics of right ventricular dysfunction in pulmonary arterial hypertension and heart failure with preserved ejection fraction. Cardiovasc Diagn Ther 2020;10:1580-603.
2. Dandel M, Hetzer R. Echocardiographic assessment of the right ventricle: Impact of the distinctly load dependency of its size, geometry and performance. Int J Cardiol 2016;221:1132-42.
3. Rako ZA, Kremer N, Yogeswaran A, et al. Adaptive versus maladaptive right ventricular remodelling. ESC Heart Fail 2023;10:762-75.
4. Lahm T, Douglas IS, Archer SL, et al. Assessment of Right Ventricular Function in the Research Setting: Knowledge Gaps and Pathways Forward. An Official American Thoracic Society Research Statement. Am J Respir Crit Care Med 2018;198:e15-43.
5. Dandel M, Potapov E, Krabatsch T, et al. Load dependency of right ventricular performance is a major factor to be considered in decision making before ventricular assist device implantation. Circulation 2013;128:S14-23.
6. Vonk Noordegraaf A, Chin KM, Haddad F, et al. Pathophysiology of the right ventricle and of the pulmonary circulation in pulmonary hypertension: an update. Eur Respir J 2019;53:1801900.
7. Kane CJ, Salama AA, Pislaru C, et al. Low Pulmonary Artery Pulsatility Index by Echocardiography Is Associated With Increased Mortality in Pulmonary Hypertension. J Am Soc Echocardiogr 2023;36:189-95.
8. Dandel M, Knosalla C, Kemper D, et al. Assessment of right ventricular adaptability to loading conditions can improve the timing of listing to transplantation in patients with pulmonary arterial hypertension. J Heart Lung Transplant 2015;34:319-28.
9. Beyls C, Huette P, Viart C, et al. Mortality of COVID-19 Patients Requiring Extracorporeal Membrane Oxygenation During the Three Epidemic Waves. ASAIO J 2022;68:1434-42.
10. Dandel M. Heart-lung interactions in COVID-19: prognostic impact and usefulness of bedside

echocardiography for monitoring of the right ventricle involvement. Heart Fail Rev 2022;27:1325-39.
11. Jordan H, Preston H, Hall DP, et al. Point-of-care echocardiography and thoracic ultrasound in the management of critically ill patients with COVID-19 infection: Experience in three regional UK intensive care units. J Intensive Care Soc 2023;24:147-53.
12. Dandel M. Pathophysiology of COVID-19-associated acute respiratory distress syndrome. Lancet Respir Med 2021;9:e4.
13. Wong SP, Otto CM. Echocardiographic findings in acute and chronic pulmonary diseases. In: Otto CM, editor. The Practice of Echocardiography. 2nd edition. Philadelphia: W.B. Saunders; 2002:739-60.
14. Pinsky MR. The right ventricle: interaction with the pulmonary circulation. Crit Care 2016;20:266.
15. Han JC, Pham T, Taberner AJ, et al. Solving a century-old conundrum underlying cardiac force-length relations. Am J Physiol Heart Circ Physiol 2019;316:H781-93.
16. Dandel M, Hetzer R. Ventricular systolic dysfunction with and without altered myocardial contractility: Clinical value of echocardiography for diagnosis and therapeutic decision-making. Int J Cardiol 2021;327:236-50.
17. Mann DI. Pathophysiology of heart failure. In: Bonow RO, Mann DL, Zipes DP, et al., editors. Braunwald's Heart Disease: A Textbook of Cardiovascular Medicine, 9th edition. Philadelphia: Elsevier Saunders; 2012:487-504.
18. Dandel M, Hetzer R. Recovery of failing hearts by mechanical unloading: Pathophysiologic insights and clinical relevance. Am Heart J 2018;206:30-50.
19. Sanz J, Sánchez-Quintana D, Bossone E, et al. Anatomy, Function, and Dysfunction of the Right Ventricle: JACC State-of-the-Art Review. J Am Coll Cardiol 2019;73:1463-82.
20. Kurtz CE. Right ventricular anatomy, function and echocardiography evaluation. In: Otto CM, editor. The Clinical Praxis of Echocardiography. 4th edition. Philadelphia: Elsevier Health Sciences; 2012:615-28.
21. Brown SB, Raina A, Katz D, et al. Longitudinal shortening accounts for the majority of right ventricular contraction and improves after pulmonary vasodilator therapy in normal subjects and patients with pulmonary arterial hypertension. Chest 2011;140:27-33.
22. Rako ZA, Yogeswaran A, Lakatos BK, et al. Clinical and functional relevance of right ventricular contraction patterns in pulmonary hypertension. J Heart Lung Transplant 2023;42:1518-28.
23. Selvetella G, Hirsch E, Notte A, et al. Adaptive and maladaptive hypertrophic pathways: points of convergence and divergence. Cardiovasc Res 2004;63:373-80.
24. Llucià-Valldeperas A, de Man FS, Bogaard HJ. Adaptation and Maladaptation of the Right Ventricle in Pulmonary Vascular Diseases. Clin Chest Med 2021;42:179-94.
25. Rain S, Andersen S, Najafi A, et al. Right Ventricular Myocardial Stiffness in Experimental Pulmonary Arterial Hypertension: Relative Contribution of Fibrosis and Myofibril Stiffness. Circ Heart Fail 2016;9:e002636.
26. Oldfield CJ, Duhamel TA, Dhalla NS. Mechanisms for the transition from physiological to pathological cardiac hypertrophy. Can J Physiol Pharmacol 2020;98:74-84.
27. Dandel M, Potapov EV, Moazami N. Preoperative evaluation of right ventricular function. In: Montalto A, Loforte A, Musumeci F, et al., editors. Mechanical circulatory support in end-stage heart failure. Switzerland: Springer Nature; 2017:75-92.
28. Cheng W, Li B, Kajstura J, et al. Stretch-induced programmed myocyte cell death. J Clin Invest 1995;96:2247-59.
29. Dandel M, Hetzer R. Temporary assist device support for the right ventricle: pre-implant and post-implant challenges. Heart Fail Rev 2018;23:157-71.
30. Naeije R, Chin K. Differentiating Precapillary From Postcapillary Pulmonary Hypertension. Circulation 2019;140:712-4.
31. Strange G, Playford D, Stewart S, et al. Pulmonary hypertension: prevalence and mortality in the Armadale echocardiography cohort. Heart 2012;98:1805-11.
32. Gotsman I, Abu Ghosh Z, Zwas DR, et al. Pulmonary Hypertension Severity in Heart Failure: Clinical Characteristics and Impact on Outcome. Am J Cardiol 2023;204:29-31.
33. Anderson JJ, Lau EM. Pulmonary Hypertension Definition, Classification, and Epidemiology in Asia. JACC Asia 2022;2:538-46.
34. Wang Z, Schreier DA, Abid H, et al. Pulmonary vascular collagen content, not cross-linking, contributes to right ventricular pulsatile afterload and overload in early pulmonary hypertension. J Appl Physiol (1985) 2017;122:253-63.
35. Grignola JC, Domingo E, López-Meseguer M, et al. Pulmonary Arterial Remodeling Is Related to the Risk Stratification and Right Ventricular-Pulmonary Arterial Coupling in Patients With Pulmonary Arterial Hypertension. Front Physiol 2021;12:631326.
36. Dandel M. Survival Benefits of Extracorporeal Membrane Oxygenation for Selected Patients With Severe

COVID-19. Ann Thorac Surg 2023;115:1085-6.
37. Zhou F, Yu T, Du R, et al. Clinical course and risk factors for mortality of adult inpatients with COVID-19 in Wuhan, China: a retrospective cohort study. Lancet 2020;395:1054-62.
38. Marini JJ, Gattinoni L. Management of COVID-19 Respiratory Distress. JAMA 2020;323:2329-30.
39. Dandel M. Etiopathogenetic Particularities and Prognostic Impact of Right Ventricular Involvement in COVID-19-Related Acute Respiratory Distress Syndrome. Crit Care Med 2022;50:e396-7.
40. Grasselli G, Greco M, Zanella A, et al. Risk Factors Associated With Mortality Among Patients With COVID-19 in Intensive Care Units in Lombardy, Italy. JAMA Intern Med 2020;180:1345-55.
41. Sawada N, Nakanishi K, Nakao T, et al. Normal Values of Echocardiographic Right Ventricular Size and Systolic Function Measurements in a Healthy Japanese Population - Subanalysis of the WASE Study. Circ Rep 2023;5:424-9.
42. van Grootel RWJ, Menting ME, McGhie J, et al. Echocardiographic chamber quantification in a healthy Dutch population. Neth Heart J 2017;25:682-90.
43. Espersen C, Skaarup KG, Lassen MCH, et al. Normal age- and sex-based values of right ventricular free wall and four-chamber longitudinal strain by speckle-tracking echocardiography: from the Copenhagen City heart study. Clin Res Cardiol 2023. doi: 10.1007/s00392-023-02333-x. [Epub ahead of print].
44. Wang TKM, Grimm RA, Rodriguez LL, et al. Defining the reference range for right ventricular systolic strain by echocardiography in healthy subjects: A meta-analysis. PLoS One 2021;16:e0256547.
45. Hosseinsabet A, Mahmoudian R, Jalali A, et al. Normal Ranges of Right Atrial Strain and Strain Rate by Two-Dimensional Speckle-Tracking Echocardiography: A Systematic Review and Meta-Analysis. Front Cardiovasc Med 2021;8:771647.
46. Dandel M, Hetzer R. Evaluation of the right ventricle by echocardiography: particularities and major challenges. Expert Rev Cardiovasc Ther 2018;16:259-75.
47. Rudski LG, Lai WW, Afilalo J, et al. Guidelines for the echocardiographic assessment of the right heart in adults: a report from the American Society of Echocardiography endorsed by the European Association of Echocardiography, a registered branch of the European Society of Cardiology, and the Canadian Society of Echocardiography. J Am Soc Echocardiogr 2010;23:685-713; quiz 786-8.
48. Leibundgut G, Rohner A, Grize L, et al. Dynamic assessment of right ventricular volumes and function by real-time three-dimensional echocardiography: a comparison study with magnetic resonance imaging in 100 adult patients. J Am Soc Echocardiogr 2010;23:116-26.
49. Forfia PR, Wiegers SE. Echocardiographic findings in acute and chronic respiratory disease. In: Otto CM, editor. The Clinical Practice of Echocardiography. 3rd edition. Philadelphia: Elsevier Health Sciences; 2007:848-76.
50. Fusini L, Tamborini G, Gripari P, et al. Feasibility of intraoperative three-dimensional transesophageal echocardiography in the evaluation of right ventricular volumes and function in patients undergoing cardiac surgery. J Am Soc Echocardiogr 2011;24:868-77.
51. Neyer J, Arsanjani R, Moriguchi J, et al. Echocardiographic parameters associated with right ventricular failure after left ventricular assist device: A review. J Heart Lung Transplant 2016;35:283-93.
52. Jorstig S, Waldenborg M, Lidén M, Thunberg P. Right ventricular ejection fraction measurements using two-dimensional transthoracic echocardiography by applying an ellipsoid model. Cardiovasc Ultrasound 2017;15:4.
53. Medvedofsky D, Mor-Avi V, Kruse E, et al. Quantification of Right Ventricular Size and Function from Contrast-Enhanced Three-Dimensional Echocardiographic Images. J Am Soc Echocardiogr 2017;30:1193-202.
54. Hamilton-Craig CR, Stedman K, Maxwell R, et al. Accuracy of quantitative echocardiographic measures of right ventricular function as compared to cardiovascular magnetic resonance. Int J Cardiol Heart Vasc 2016;12:38-44.
55. Park JB, Lee SP, Lee JH, et al. Quantification of Right Ventricular Volume and Function Using Single-Beat Three-Dimensional Echocardiography: A Validation Study with Cardiac Magnetic Resonance. J Am Soc Echocardiogr 2016;29:392-401.
56. Dandel M. Potential Impact of Tricuspid and Mitral Valve Regurgitation on the Diagnostic and Prognostic Value of Ventricular Ejection Fraction. J Am Soc Echocardiogr 2020;33:518.
57. Anavekar NS, Gerson D, Skali H, et al. Two-dimensional assessment of right ventricular function: an echocardiographic-MRI correlative study. Echocardiography 2007;24:452-6.
58. Atsumi A, Ishizu T, Kameda Y, et al. Application of 3-dimensional speckle tracking imaging to the assessment of right ventricular regional deformation. Circ J 2013;77:1760-8.

59. DiLorenzo MP, Bhatt SM, Mercer-Rosa L. How best to assess right ventricular function by echocardiography. Cardiol Young 2015;25:1473-81.
60. Jurcut R, Giusca S, La Gerche A, et al. The echocardiographic assessment of the right ventricle: what to do in 2010?. Eur J Echocardiogr 2010;11:81-96.
61. Focardi M, Cameli M, Carbone SF, et al. Traditional and innovative echocardiographic parameters for the analysis of right ventricular performance in comparison with cardiac magnetic resonance. Eur Heart J Cardiovasc Imaging 2015;16:47-52.
62. Hsiao SH, Lin SK, Wang WC, et al. Severe tricuspid regurgitation shows significant impact in the relationship among peak systolic tricuspid annular velocity, tricuspid annular plane systolic excursion, and right ventricular ejection fraction. J Am Soc Echocardiogr 2006;19:902-10.
63. Flo Forner A, Hasheminejad E, Sabate S, et al. Agreement of tricuspid annular systolic excursion measurement between transthoracic and transesophageal echocardiography in the perioperative setting. Int J Cardiovasc Imaging 2017;33:1385-94.
64. Allam LE, Onsy AM, Ghalib HA. Right Ventricular Outflow Tract Systolic Excursion and Fractional Shortening: Can These Echocardiographic Parameters be Used for the Assessment of Right Ventricular Function? J Cardiovasc Echogr 2017;27:52-8.
65. Lindqvist P, Henein M, Kazzam E. Right ventricular outflow-tract fractional shortening: an applicable measure of right ventricular systolic function. Eur J Echocardiogr 2003;4:29-35.
66. Kanzaki H, Nakatani S, Kawada T, et al. Right ventricular dP/dt/P(max), not dP/dt(max), noninvasively derived from tricuspid regurgitation velocity is a useful index of right ventricular contractility. J Am Soc Echocardiogr 2002;15:136-42.
67. Blanchard DG, Malouf PJ, Gurudevan SV, et al. Utility of right ventricular Tei index in the noninvasive evaluation of chronic thromboembolic pulmonary hypertension before and after pulmonary thromboendarterectomy. JACC Cardiovasc Imaging 2009;2:143-9.
68. Yoshifuku S, Otsuji Y, Takasaki K, et al. Pseudonormalized Doppler total ejection isovolume (Tei) index in patients with right ventricular acute myocardial infarction. Am J Cardiol 2003;91:527-31.
69. Topilsky Y, Oh JK, Shah DK, et al. Echocardiographic predictors of adverse outcomes after continuous left ventricular assist device implantation. JACC Cardiovasc Imaging 2011;4:211-22.
70. Dandel M, Lehmkuhl H, Knosalla C, et al. Strain and strain rate imaging by echocardiography - basic concepts and clinical applicability. Curr Cardiol Rev 2009;5:133-48.
71. Kukulski T, Hübbert L, Arnold M, et al. Normal regional right ventricular function and its change with age: a Doppler myocardial imaging study. J Am Soc Echocardiogr 2000;13:194-204.
72. Lindqvist P, Waldenström A, Wikström G, et al. The use of isovolumic contraction velocity to determine right ventricular state of contractility and filling pressures A pulsed Doppler tissue imaging study. Eur J Echocardiogr 2005;6:264-70.
73. Chrysohoou C, Antoniou CK, Kotrogiannis I, et al. Role of right ventricular systolic function on long-term outcome in patients with newly diagnosed systolic heart failure. Circ J 2011;75:2176-81.
74. Haddad F, Hunt SA, Rosenthal DN, et al. Right ventricular function in cardiovascular disease, part I: Anatomy, physiology, aging, and functional assessment of the right ventricle. Circulation 2008;117:1436-48.
75. Longobardo L, Suma V, Jain R, et al. Role of Two-Dimensional Speckle-Tracking Echocardiography Strain in the Assessment of Right Ventricular Systolic Function and Comparison with Conventional Parameters. J Am Soc Echocardiogr 2017;30:937-46.e6.
76. Kemal HS, Kayikcioglu M, Kultursay H, et al. Right ventricular free-wall longitudinal speckle tracking strain in patients with pulmonary arterial hypertension under specific treatment. Echocardiography 2017;34:530-6.
77. Park JH, Negishi K, Kwon DH, et al. Validation of global longitudinal strain and strain rate as reliable markers of right ventricular dysfunction: comparison with cardiac magnetic resonance and outcome. J Cardiovasc Ultrasound 2014;22:113-20.
78. Motoki H, Borowski AG, Shrestha K, et al. Right ventricular global longitudinal strain provides prognostic value incremental to left ventricular ejection fraction in patients with heart failure. J Am Soc Echocardiogr 2014;27:726-32.
79. Boegershausen N, Zayat R, Aljalloud A, et al. Risk factors for the development of right ventricular failure after left ventricular assist device implantation-a single-centre retrospective with focus on deformation imaging. Eur J Cardiothorac Surg 2017;52:1069-76.
80. Kong D, Shu X, Dong L, et al. Right ventricular regional systolic function and dyssynchrony in patients with pulmonary hypertension evaluated by three-dimensional echocardiography. J Am Soc Echocardiogr

2013;26:649-56.
81. Badagliacca R, Reali M, Poscia R, et al. Right Intraventricular Dyssynchrony in Idiopathic, Heritable, and Anorexigen-Induced Pulmonary Arterial Hypertension: Clinical Impact and Reversibility. JACC Cardiovasc Imaging 2015;8:642-52.
82. Werther Evaldsson A, Ingvarsson A, Waktare J, et al. Right ventricular speckle tracking assessment for differentiation of pressure- versus volume-overloaded right ventricle. Clin Physiol Funct Imaging 2018;38:763-71.
83. Ishizu T, Seo Y, Atsumi A, et al. Global and Regional Right Ventricular Function Assessed by Novel Three-Dimensional Speckle-Tracking Echocardiography. J Am Soc Echocardiogr 2017;30:1203-13.
84. Cameli M, Lisi M, Mondillo S, et al. Prediction of stroke volume by global left ventricular longitudinal strain in patients undergoing assessment for cardiac transplantation. J Crit Care 2011;26:433.e13-20.
85. Cameli M, Bernazzali S, Lisi M, et al. Right ventricular longitudinal strain and right ventricular stroke work index in patients with severe heart failure: left ventricular assist device suitability for transplant candidates. Transplant Proc 2012;44:2013-5.
86. Bellavia D, Iacovoni A, Scardulla C, et al. Prediction of right ventricular failure after ventricular assist device implant: systematic review and meta-analysis of observational studies. Eur J Heart Fail 2017;19:926-46.
87. Wright L, Negishi K, Dwyer N, et al. Afterload Dependence of Right Ventricular Myocardial Strain. J Am Soc Echocardiogr 2017;30:676-684.e1.
88. Park JH, Kusunose K, Kwon DH, et al. Relationship between Right Ventricular Longitudinal Strain, Invasive Hemodynamics, and Functional Assessment in Pulmonary Arterial Hypertension. Korean Circ J 2015;45:398-407.
89. Jasaityte R, Dandel M, Lehmkuhl H, et al. Prediction of short-term outcomes in patients with idiopathic dilated cardiomyopathy referred for transplantation using standard echocardiography and strain imaging. Transplant Proc 2009;41:277-80.
90. Yu HC, Sanderson JE. Different prognostic significance of right and left ventricular diastolic dysfunction in heart failure. Clin Cardiol 1999;22:504-12.
91. Sallach JA, Tang WH, Borowski AG, et al. Right atrial volume index in chronic systolic heart failure and prognosis. JACC Cardiovasc Imaging 2009;2:527-34.
92. Henning RJ. Tricuspid valve regurgitation: current diagnosis and treatment. Am J Cardiovasc Dis 2022;12:1-18.
93. Hahn RT, Thomas JD, Khalique OK, et al. Imaging Assessment of Tricuspid Regurgitation Severity. JACC Cardiovasc Imaging 2019;12:469-90.
94. Hahn RT, Badano LP, Bartko PE, et al. Tricuspid regurgitation: recent advances in understanding pathophysiology, severity grading and outcome. Eur Heart J Cardiovasc Imaging 2022;23:913-29.
95. Dandel M, Krabatsch T, Falk V. Left ventricular vs. biventricular mechanical support: Decision making and strategies for avoidance of right heart failure after left ventricular assist device implantation. Int J Cardiol 2015;198:241-50.
96. Amsallem M, Boulate D, Aymami M, et al. Load Adaptability in Patients With Pulmonary Arterial Hypertension. Am J Cardiol 2017;120:874-82.
97. Sharma J, Bhise M, Singh A, et al. Hemodynamic measurements after cardiac surgery: transesophageal Doppler versus pulmonary artery catheter. J Cardiothorac Vasc Anesth 2005;19:746-50. Erratum in: J Cardiothorac Vasc Anesth 2008;22:339.
98. Gumus F, Durdu MS, Cakici M, et al. Right ventricular free wall longitudinal strain and stroke work index for predicting right heart failure after left ventricular assist device therapy. Interact Cardiovasc Thorac Surg 2019;28:674-82.
99. Frea S, Bovolo V, Bergerone S, et al. Echocardiographic evaluation of right ventricular stroke work index in advanced heart failure: a new index? J Card Fail 2012;18:886-93.
100. Di Maria MV, Burkett DA, Younoszai AK, et al. Echocardiographic estimation of right ventricular stroke work in children with pulmonary arterial hypertension: comparison with invasive measurements. J Am Soc Echocardiogr 2015;28:1350-7.
101. Frea S, Pidello S, Bovolo V, et al. Prognostic incremental role of right ventricular function in acute decompensation of advanced chronic heart failure. Eur J Heart Fail 2016;18:564-72.
102. Kalenderoğlu K, Güvenç TS, Mete MT, et al. Usefulness of right ventricular contraction pressure index to predict short-term mortality and right heart failure in patients who underwent continuous-flow left ventricular assist device implantation. Int J Artif Organs 2020;43:25-36.
103. Guazzi M, Bandera F, Pelissero G, et al. Tricuspid annular plane systolic excursion and pulmonary arterial systolic pressure relationship in heart failure: an index of right ventricular contractile function and prognosis. Am J Physiol Heart Circ Physiol 2013;305:H1373-81.

104. López-Candales A, Lopez FR, Trivedi S, et al. Right ventricular ejection efficiency: a new echocardiographic measure of mechanical performance in chronic pulmonary hypertension. Echocardiography 2014;31:516-23.
105. Guazzi M, Naeije R, Arena R, et al. Echocardiography of Right Ventriculoarterial Coupling Combined With Cardiopulmonary Exercise Testing to Predict Outcome in Heart Failure. Chest 2015;148:226-34.
106. Guazzi M, Dixon D, Labate V, et al. RV Contractile Function and its Coupling to Pulmonary Circulation in Heart Failure With Preserved Ejection Fraction: Stratification of Clinical Phenotypes and Outcomes. JACC Cardiovasc Imaging 2017;10:1211-21.
107. Rajagopal S, Forsha DE, Risum N, et al. Comprehensive assessment of right ventricular function in patients with pulmonary hypertension with global longitudinal peak systolic strain derived from multiple right ventricular views. J Am Soc Echocardiogr 2014;27:657-665.e3.
108. Abbas AE, Franey LM, Marwick T, et al. Noninvasive assessment of pulmonary vascular resistance by Doppler echocardiography. J Am Soc Echocardiogr 2013;26:1170-7.
109. Naeije R, Manes A. The right ventricle in pulmonary arterial hypertension. Eur Respir Rev 2014;23:476-87.
110. Ryo K, Goda A, Onishi T, et al. Characterization of right ventricular remodeling in pulmonary hypertension associated with patient outcomes by 3-dimensional wall motion tracking echocardiography. Circ Cardiovasc Imaging 2015;8:e003176.
111. Porter TR, Shillcutt SK, Adams MS, et al. Guidelines for the use of echocardiography as a monitor for therapeutic intervention in adults: a report from the American Society of Echocardiography. J Am Soc Echocardiogr 2015;28:40-56.
112. Dandel M, Hetzer R. Echocardiographic Assessment of the Right-Sided Heart for Surveillance of Patients With Pulmonary Arterial Hypertension. JACC Cardiovasc Imaging 2019;12:764-6.
113. Landra F, Sciaccaluga C, Pastore MC, et al. Right ventricular myocardial work for the prediction of early right heart failure and long-term mortality after left ventricular assist device implant. Eur Heart J Cardiovasc Imaging 2023;25:105-15.
114. Dang NC, Topkara VK, Mercando M, et al. Right heart failure after left ventricular assist device implantation in patients with chronic congestive heart failure. J Heart Lung Transplant 2006;25:1-6.
115. Dandel M, Weng Y, Siniawski H, et al. Heart failure reversal by ventricular unloading in patients with chronic cardiomyopathy: criteria for weaning from ventricular assist devices. Eur Heart J 2011;32:1148-60.
116. Ramberg E, Olausson M, Jørgensen TB, et al. Right atrial and ventricular function evaluated with speckle tracking in patients with acute pulmonary embolism. Am J Emerg Med 2017;35:136-43.
117. Fields JM, Davis J, Girson L, et al. Transthoracic Echocardiography for Diagnosing Pulmonary Embolism: A Systematic Review and Meta-Analysis. J Am Soc Echocardiogr 2017;30:714-723.e4.
118. Dandel M, Hetzer R. Role of echocardiography in selection, implantation, and management of left ventricular assist device therapy. In: Sawyer DB, Vasan RS, editors. Encyclopedia of Cardiovascular Research and Medicine. Elsevier; 2018:327-44.
119. Al Ateah G, Kirschfink A, Frick M, et al. Echocardiographic determination of right ventricular volumes and ejection fraction: Validation of a truncated cone and rhomboid pyramid formula. PLoS One 2023;18:e0290418.
120. Seo J, Hong YJ, Batbayar U, et al. Prognostic value of functional tricuspid regurgitation quantified by cardiac magnetic resonance in heart failure. Eur Heart J Cardiovasc Imaging 2023;24:742-50.
121. Matthews JC, Koelling TM, Pagani FD, et al. The right ventricular failure risk score a pre-operative tool for assessing the risk of right ventricular failure in left ventricular assist device candidates. J Am Coll Cardiol 2008;51:2163-72.
122. Ochiai Y, McCarthy PM, Smedira NG, et al. Predictors of severe right ventricular failure after implantable left ventricular assist device insertion: analysis of 245 patients. Circulation 2002;106:I198-I202.
123. Dandel M. Role of Echocardiography in the Management of Patients with Advanced (Stage D) Heart Failure Related to Nonischemic Cardiomyopathy. Rev Cardiovasc Med 2022;23:214.
124. Potapov EV, Stepanenko A, Dandel M, et al. Tricuspid incompetence and geometry of the right ventricle as predictors of right ventricular function after implantation of a left ventricular assist device. J Heart Lung Transplant 2008;27:1275-81.
125. Miller LW, Russel SD. Candidate selection for long-term left ventricular assist device therapy for advanced heart failure. In: Kormos RL, Miller LW, editors. Mechanical Circulatory Support: A Companion to Braunwald's Heart Disease. Philadelphia: Elsevier Saunders; 2012:72-87.
126. Kukucka M, Potapov E, Stepanenko A, et al. Acute

impact of left ventricular unloading by left ventricular assist device on the right ventricle geometry and function: effect of nitric oxide inhalation. J Thorac Cardiovasc Surg 2011;141:1009-14.
127. Fukamachi K, McCarthy PM, Smedira NG, et al. Preoperative risk factors for right ventricular failure after implantable left ventricular assist device insertion. Ann Thorac Surg 1999;68:2181-4.
128. Baumwol J, Macdonald PS, Keogh AM, et al. Right heart failure and "failure to thrive" after left ventricular assist device: clinical predictors and outcomes. J Heart Lung Transplant 2011;30:888-95.
129. Santambrogio L, Bianchi T, Fuardo M, et al. Right ventricular failure after left ventricular assist device insertion: preoperative risk factors. Interact Cardiovasc Thorac Surg 2006;5:379-82.
130. Puwanant S, Hamilton KK, Klodell CT, et al. Tricuspid annular motion as a predictor of severe right ventricular failure after left ventricular assist device implantation. J Heart Lung Transplant 2008;27:1102-7.
131. Kato TS, Farr M, Schulze PC, et al. Usefulness of two-dimensional echocardiographic parameters of the left side of the heart to predict right ventricular failure after left ventricular assist device implantation. Am J Cardiol 2012;109:246-51.
132. Raina A, Seetha Rammohan HR, et al. Postoperative right ventricular failure after left ventricular assist device placement is predicted by preoperative echocardiographic structural, hemodynamic, and functional parameters. J Card Fail 2013;19:16-24.
133. Grant AD, Smedira NG, Starling RC, et al. Independent and incremental role of quantitative right ventricular evaluation for the prediction of right ventricular failure after left ventricular assist device implantation. J Am Coll Cardiol 2012;60:521-8.
134. Imamura T, Kinugawa K, Kato N, et al. Late-onset right ventricular failure in patients with preoperative small left ventricle after implantation of continuous flow left ventricular assist device. Circ J 2014;78:625-33.
135. Charisopoulou D, Banner NR, Demetrescu C, et al. Right atrial and ventricular echocardiographic strain analysis predicts requirement for right ventricular support after left ventricular assist device implantation. Eur Heart J Cardiovasc Imaging 2019;20:199-208.
136. Aissaoui N, Salem JE, Paluszkiewicz L, et al. Assessment of right ventricular dysfunction predictors before the implantation of a left ventricular assist device in end-stage heart failure patients using echocardiographic measures (ARVADE): Combination of left and right ventricular echocardiographic variables. Arch Cardiovasc Dis. 2015;108:300-9.
137. Atluri P, Goldstone AB, Fairman AS, et al. Predicting right ventricular failure in the modern, continuous flow left ventricular assist device era. Ann Thorac Surg 2013;96:857-63; discussion 863-4.
138. Vivo RP, Cordero-Reyes AM, Qamar U, et al. Increased right-to-left ventricle diameter ratio is a strong predictor of right ventricular failure after left ventricular assist device. J Heart Lung Transplant. 2013;32:792-9.
139. Kato TS, Jiang J, Schulze PC, et al. Serial echocardiography using tissue Doppler and speckle tracking imaging to monitor right ventricular failure before and after left ventricular assist device surgery. JACC Heart Fail 2013;1:216-22.
140. Fitzpatrick JR 3rd, Frederick JR, Hsu VM, et al. Risk score derived from pre-operative data analysis predicts the need for biventricular mechanical circulatory support. J Heart Lung Transplant. 2008;27:1286-92.
141. Goldraich L, Kawajiri H, Foroutan F, et al. Tricuspid Valve Annular Dilation as a Predictor of Right Ventricular Failure After Implantation of a Left Ventricular Assist Device. J Card Surg 2016;31:110-6.
142. Liang LW, Jamil A, Mazurek JA, et al. Right Ventricular Global Longitudinal Strain as a Predictor of Acute and Early Right Heart Failure Post Left Ventricular Assist Device Implantation. ASAIO J 2022;68:333-9.
143. Kalogeropoulos AP, Al-Anbari R, Pekarek A, et al. The Right Ventricular Function After Left Ventricular Assist Device (RVF-LVAD) study: rationale and preliminary results. Eur Heart J Cardiovasc Imaging 2016;17:429-37.
144. Redlin M, Miera O, Habazettl H, et al. Incidence and echocardiographic predictors of early postoperative right ventricular dysfunction following left ventricular assist implantation in paediatric patients. Interact Cardiovasc Thorac Surg 2017;25:887-91.
145. Kiernan MS, French AL, DeNofrio D, et al. Preoperative three-dimensional echocardiography to assess risk of right ventricular failure after left ventricular assist device surgery. J Card Fail 2015;21:189-97.
146. Nakanishi K, Homma S, Han J, et al. Usefulness of Tricuspid Annular Diameter to Predict Late Right Sided Heart Failure in Patients With Left Ventricular Assist Device. Am J Cardiol 2018;122:115-20.
147. Cameli M, Loiacono F, Sparla S, et al. Systematic Left Ventricular Assist Device Implant Eligibility with Non-Invasive Assessment: The SIENA Protocol. J Cardiovasc

Ultrasound 2017;25:39-46.
148. Rodenas-Alesina E, Brahmbhatt DH, Rao V, et al. Prediction, prevention, and management of right ventricular failure after left ventricular assist device implantation: A comprehensive review. Front Cardiovasc Med 2022;9:1040251.
149. Dandel M, Javier MFDM, Javier Delmo EMD, et al. Accurate assessment of right heart function before and after long-term left ventricular assist device implantation. Expert Rev Cardiovasc Ther 2020;18:289-308.
150. Amsallem M, Aymami M, Hiesinger W, et al. Right ventricular load adaptability metrics in patients undergoing left ventricular assist device implantation. J Thorac Cardiovasc Surg 2019;157:1023-1033.e4.
151. Vonk-Noordegraaf A, Haddad F, Chin KM, et al. Right heart adaptation to pulmonary arterial hypertension: physiology and pathobiology. J Am Coll Cardiol 2013;62:D22-33.
152. Benza RL, Miller DP, Gomberg-Maitland M, et al. Predicting survival in pulmonary arterial hypertension: insights from the Registry to Evaluate Early and Long-Term Pulmonary Arterial Hypertension Disease Management (REVEAL). Circulation 2010;122:164-72.
153. Humbert M, Sitbon O, Chaouat A, et al. Survival in patients with idiopathic, familial, and anorexigen-associated pulmonary arterial hypertension in the modern management era. Circulation 2010;122:156-63.
154. Campo A, Mathai SC, Le Pavec J, et al. Outcomes of hospitalisation for right heart failure in pulmonary arterial hypertension. Eur Respir J 2011;38:359-67.
155. Haddad F, Peterson T, Fuh E, et al. Characteristics and outcome after hospitalization for acute right heart failure in patients with pulmonary arterial hypertension. Circ Heart Fail 2011;4:692-9.
156. Rich S. Pulmonary Hypertension. In: Bonow RO, Mann DL, Zipes DP, et al., editors. Braunwald's Heart Disease: A Textbook of Cardiovascular Medicine. 9th ed. Philadelphia: Elsevier Saunders; 2012;1696-718.
157. D'Alonzo GE, Barst RJ, Ayres SM, et al. Survival in patients with primary pulmonary hypertension. Results from a national prospective registry. Ann Intern Med 1991;115:343-9.
158. Miller DP, Farber HW. "Who'll be the next in line?" The lung allocation score in patients with pulmonary arterial hypertension. J Heart Lung Transplant 2013;32:1165-7.
159. McLaughlin VV, Gaine SP, Howard LS, et al. Treatment goals of pulmonary hypertension. J Am Coll Cardiol 2013;62:D73-81.
160. Chandra S, Shah SJ, Thenappan T, et al. Carbon monoxide diffusing capacity and mortality in pulmonary arterial hypertension. J Heart Lung Transplant 2010;29:181-7.
161. Sato T, Tsujino I, Ohira H, et al. Validation study on the accuracy of echocardiographic measurements of right ventricular systolic function in pulmonary hypertension. J Am Soc Echocardiogr 2012;25:280-6.
162. Spruijt OA, Di Pasqua MC, Bogaard HJ, et al. Serial assessment of right ventricular systolic function in patients with precapillary pulmonary hypertension using simple echocardiographic parameters: A comparison with cardiac magnetic resonance imaging. J Cardiol 2017;69:182-8.
163. Amsallem M, Sweatt AJ, Aymami MC, et al. Right Heart End-Systolic Remodeling Index Strongly Predicts Outcomes in Pulmonary Arterial Hypertension: Comparison With Validated Models. Circ Cardiovasc Imaging 2017;10:e005771.
164. Ghio S, Pazzano AS, Klersy C, et al. Clinical and prognostic relevance of echocardiographic evaluation of right ventricular geometry in patients with idiopathic pulmonary arterial hypertension. Am J Cardiol 2011;107:628-32.
165. Zhang R, Dai LZ, Xie WP, et al. Survival of Chinese patients with pulmonary arterial hypertension in the modern treatment era. Chest 2011;140:301-9.
166. Raymond RJ, Hinderliter AL, Willis PW, et al. Echocardiographic predictors of adverse outcomes in primary pulmonary hypertension. J Am Coll Cardiol 2002;39:1214-9.
167. Yeo TC, Dujardin KS, Tei C, et al. Value of a Doppler-derived index combining systolic and diastolic time intervals in predicting outcome in primary pulmonary hypertension. Am J Cardiol 1998;81:1157-61.
168. Ernande L, Cottin V, Leroux PY, et al. Right isovolumic contraction velocity predicts survival in pulmonary hypertension. J Am Soc Echocardiogr 2013;26:297-306.
169. Fine NM, Chen L, Bastiansen PM, et al. Outcome prediction by quantitative right ventricular function assessment in 575 subjects evaluated for pulmonary hypertension. Circ Cardiovasc Imaging 2013;6:711-21.
170. Bustamante-Labarta M, Perrone S, De La Fuente RL, et al. Right atrial size and tricuspid regurgitation severity predict mortality or transplantation in primary pulmonary hypertension. J Am Soc Echocardiogr 2002;15:1160-4.
171. Forfia PR, Fisher MR, Mathai SC, et al. Tricuspid annular displacement predicts survival in pulmonary hypertension. Am J Respir Crit Care Med 2006;174:1034-41.
172. López-Candales A, Dohi K, Rajagopalan N, et al. Right

ventricular dyssynchrony in patients with pulmonary hypertension is associated with disease severity and functional class. Cardiovasc Ultrasound 2005;3:23.
173. Okumura K, Humpl T, Dragulescu A, et al. Longitudinal assessment of right ventricular myocardial strain in relation to transplant-free survival in children with idiopathic pulmonary hypertension. J Am Soc Echocardiogr 2014;27:1344-51.
174. Crossman LM, Rajaram P, Hart CM, et al. Evaluation of right ventricular strain in two separate cohorts with precapillary pulmonary hypertension. Pulm Circ 2023;13:e12204.
175. Giusca S, Jurcut R, Coman IM, et al. Right ventricular function predicts clinical response to specific vasodilator therapy in patients with pulmonary hypertension. Echocardiography 2013;30:17-26.
176. Kusunose K, Tsutsui RS, Bhatt K, et al. Prognostic value of RV function before and after lung transplantation. JACC Cardiovasc Imaging 2014;7:1084-94.
177. Cheng XL, Liu BY, Wu WC, et al. Impact of right ventricular dyssynchrony on prognosis of patients with idiopathic pulmonary arterial hypertension. Pulm Circ 2019;9:2045894019883609.
178. von Siebenthal C, Aubert JD, Mitsakis P, et al. Pulmonary Hypertension and Indicators of Right Ventricular Function. Front Med (Lausanne) 2016;3:23.
179. Murata M, Tsugu T, Kawakami T, et al. Right ventricular dyssynchrony predicts clinical outcomes in patients with pulmonary hypertension. Int J Cardiol 2017;228:912-8.
180. Dandel M. Cardiac manifestations of COVID-19 infection: the role of echocardiography in patient management. Infection 2021;49:187-9.
181. Gorder K, Young W, Kapur NK, et al. Mechanical Circulatory Support in COVID-19. Cardiol Clin 2022;40:329-35.
182. Norderfeldt J, Liliequist A, Frostell C, et al. Acute pulmonary hypertension and short-term outcomes in severe Covid-19 patients needing intensive care. Acta Anaesthesiol Scand 2021;65:761-9.
183. Vonk Noordegraaf A, Westerhof BE, Westerhof N. The Relationship Between the Right Ventricle and its Load in Pulmonary Hypertension. J Am Coll Cardiol 2017;69:236-43.
184. Dandel M. Echocardiography Can Improve the Selection of Mechanical Support Strategies for Patients With Severe COVID-19 Respiratory Distress Syndrome. ASAIO J 2023;69:e418.
185. Fox SE, Akmatbekov A, Harbert JL, et al. Pulmonary and cardiac pathology in African American patients with COVID-19: an autopsy series from New Orleans. Lancet Respir Med 2020;8:681-6.
186. Dolhnikoff M, Duarte-Neto AN, de Almeida Monteiro RA, et al. Pathological evidence of pulmonary thrombotic phenomena in severe COVID-19. J Thromb Haemost 2020;18:1517-9.
187. Ackermann M, Verleden SE, Kuehnel M, et al. Pulmonary Vascular Endothelialitis, Thrombosis, and Angiogenesis in Covid-19. N Engl J Med 2020;383:120-8.
188. Carsana L, Sonzogni A, Nasr A, et al. Pulmonary post-mortem findings in a series of COVID-19 cases from northern Italy: a two-centre descriptive study. Lancet Infect Dis 2020;20:1135-40.
189. Wichmann D, Sperhake JP, Lütgehetmann M, et al. Autopsy Findings and Venous Thromboembolism in Patients With COVID-19: A Prospective Cohort Study. Ann Intern Med 2020;173:268-77.
190. Greyson C, Xu Y, Lu L, et al. Right ventricular pressure and dilation during pressure overload determine dysfunction after pressure overload. Am J Physiol Heart Circ Physiol 2000;278:H1414-20.
191. Chotalia M, Ali M, Alderman JE, et al. Right Ventricular Dysfunction and Its Association With Mortality in Coronavirus Disease 2019 Acute Respiratory Distress Syndrome. Crit Care Med 2021;49:1757-68.
192. McFadyen JD, Stevens H, Peter K. The Emerging Threat of (Micro)Thrombosis in COVID-19 and Its Therapeutic Implications. Circ Res 2020;127:571-87.
193. McErlane J, McCall P, Willder J, et al. Right ventricular free wall longitudinal strain is independently associated with mortality in mechanically ventilated patients with COVID-19. Ann Intensive Care 2022;12:104.
194. Dandel M. Timely Identification of Hospitalized Patients at Risk for COVID-19-Associated Right Heart Failure Should Be a Major Goal of Echocardiographic Surveillance. J Am Soc Echocardiogr 2021;34:1323.

Cite this article as: Dandel M. Monitoring of the right ventricular responses to pressure overload: prognostic value and usefulness of echocardiography for clinical decision-making. Cardiovasc Diagn Ther 2024;14(1):193-222. doi: 10.21037/cdt-23-380

